Flat singularities of chained systems, illustrated with an aircraft model

Yirmeyahu Kaminski, François Ollivier

FLAT SINGULARITIES OF CHAINED SYSTEMS, ILLUSTRATED WITH AN AIRCRAFT MODEL

A PREPRINT

Yirmeyahu J. Kaminski
Holon Institute of Technology
Holon, Israel
kaminsj@hit.ac.il

François Ollivier
LIX, CNRS–École Polytechnique
91128 Palaiseau Cedex, France
ollivier@lix.polytechnique.fr

August 23, 2022

ABSTRACT

We investigate apparent and intrinsic singularities of block diagonal systems. These systems admit a partition of the set of state functions $\Xi = \bigcup_{i=1}^{r} \Xi_i$, such that derivatives of a state variable in Ξ_i only depend on state variables in $\Xi_1, \ldots, \Xi_{i+1}$. They include various notions of ĉhained systems*.* Such systems are flat in the generic case, which means that their solutions may be parametrized by a finite set of differentially independent functions, called *flat outputs* and a finite number of their derivatives, provided that some Jacobian determinant does not vanish.

Using theoretical results related to Jacobi's bound, flatness conditions can be reduced to the non vanishing of Jacobi's *truncated determinant*. An algorithm is provided to test if a system is block diagonal.

We illustrate such systems with a study of a simplified aircraft model. We exhibit new sets of flat outputs, provide explicit regularity conditions for them and interpret some flat singularities as stalling conditions. This simplified model remains flat using some alternative controls such as differential thrust in case of rudder failure, or when one or all engines are lost.

We conclude this work with numerical simulation showing that a feed-back using those fkat outputs is robust to perturbations and can also compensate model errors, when using a more realistic aerodynamic model.

RÉSUMÉ

Nous étudions les singularités intrinsèques et apparentes des systèmes diagonaux par blocs. Ces systèmes admettent un partition de l'ensemble des fonction d'état $\Xi = \bigcup_{i=1}^{r} \Xi_i$, telle que les dérivées des variables d'état de Ξ_i dépendent uniquement des variables d'état de $\Xi_1, \ldots, \Xi_{i+1}$. Ils incluent différentes notions de "systèmes chaînés". Ils sont plats dans le cas générique, c'est-à-dire que leurs solutions peuvent être paramétrées en utilisant des fonctions d'état, appelées *sorties plates* et un nombre fini de leurs dérivées, pourvu qu'un déterminant jacobien ne s'annule pas.

Des résultats théoriques provenant de la Borne de Jacobi et de la réduction en forme normale la plus courte, les conditions de platitude se ramènent à la non nullité du *déterminant tronqué* de Jacobi. Nous décrivons un algorithme permettant de tester si un système est diagonal par bloc. Un condition nécessaire de platitude est également donnée.

Nous illustrons ces systèmes par l'étude d'un modèle d'avion simplifié. De nouveaux ensembles de sorties linéarisantes sont décrits, ainsi que des conditions explicites de régularité. Certaines singularités plates sont interprètées comme des situations de décrochage. Ce modèle simplifié demeure plat en utilisant des fonctions de contrôle alternatives comme la poussée différentielle en cas de panne de gouvernail, ou lorsque tous les moteurs sont en panne.

Nous concluons ce travail avec des simulations numériques montrant qu'un bouclage utilisant ces sorties linéarisante est robuste aux perturbations et peut compenser aussi les erreurs de modèles lorsque l'on utilise un modèle aérodynamique plus réaliste.

AMS classifiaction: 93-10, 93B27, 93D15, 68W30, 12H05, 90C27

Key words: differentially flat systems, flat singularities, flat outputs, aircraft aerodynamics models, gravity-free flight, engine failure, rudder jam, differential thrust, forward sleep landing, Jacobi's bound, Hungarian method

1 Introduction

1.1 Aims of this paper

We continue the investigation of intrinsic and apparent singularities of flat control system [8, 9, 24, 25], initiated in our previous papers [16, 17], with a study of block triangular systems that generalizes *extended chained form* [12] and an application to aircraft control. We recall that flat systems are systems for which the trajectory can be parametrized using a finite set of state functions, call *flat outputs*, and a finite number of their derivatives.

The class of block triangular system is important in practice as it includes various notions of "chained systems", containing many classical examples such as robot arms [10, 38], cars with many trailers [36] or discretizations of PDE flat systems [35, 37]. For them, testing flatness reduces to computing the rank of Jacobian matrices and finding the flat outputs to an easy combinatorial problem.

Our goal is to investigate all the related possible choices of flat outputs and their singularity conditions. These theoretical results are illustrated with a study of a simplified aircraft model.

1.2 Main theoretical results

Block diagonal systems as systems such that derivatives of state variable in Ξ_i, for $1 \leq i < r$ only depend on state variables in $\Xi_1, \ldots, \Xi_{i+1}$. We characterize such systems and their associated flat outputs using Jacobi's bound [31]. Jacobi's bound is a bound on the order of a system of n equation P_i in n variables x_i, which is expressed as the tropical determinant of the order matrix $A_P = (\mathrm{ord}_{x_j} P_i)$. To achieve flat parametrization, we assign to each flat output $x \in Z$ a time trajectory ζ_x. Possible flat outputs Z are such that Jacobi's bound of the system P_i, $x - \zeta_x(t)$, for $x \in Z$ is 0 and its truncated determinant does not identically vanish, which implies that the parametrization can be computed.

We provide an algorithm that works in polynomial time in the number of state variables to test if a system is block diagonal and find possible choices of flat outputs.

1.3 Flat outputs for the aircraft and regularity conditions

Martin has shown that a simplified aircraft model where the thrusts related to the actuators and angular velocities are neglected is flat and given the flat output x, y, z, β, where (x, y, z) are the coordinates of the center of gravity and β the sideslip angle. We show that the bank angle μ, the angle of attack α and the engine thrust F can also be used instead of β.

We explicit regularity conditions for those choices of flat outputs and show that the regularity condition for μ is related to some kind of stalling condition.

1.4 Numerical simulations, models and implementations

In our simulations, we used the aircraft model and sets of parameters provided by Grauer and Morelli [11] for various types of aircraft: fighter F16C, STOL utility aircraft DHC-6 Twin Otter and NASA Generic Transport Model (GTM), a subscale airliner model. Such aerodynamics models are not known to be flat, unless one neglects some terms, such as the thrusts created by the control surfaces (ailerons, elevators, rudder) or related to angular speeds.

We investigated first the robustness of the flat control with respect to some failures and some perturbations, for the simplified model, using simulations performed in Python. In a second stage, a Maple implementation was used to test the ability of a suitable feed-back to keep the trajectories of the full model close to the theoretical trajectories computed with the simplified flat one.

We investigate flight situations near intrinsic singularities, that correspond basically to stalling, and apparent singularities, such as gravity-free flight, for which we use alternative flat outputs, including bank angle μ. We also show that a set of flat outputs including the thrust F may be used when $\beta \neq 0$ and is suitable to control a slip-forward maneuver for dead-stick emergency landing [3, 4].

When control surfaces are lost or actuators damaged, alternative controls may be used [5, 6, 14, 23]. We have investigated the use of differential thrust in the case of a damaged rudder.

1.5 Plan of the paper

In sec. 2, we define flatness and flat singularities 2.1. In sec. 3, we present elementary results related to Jacobi's bound 3.1 before defininining block triangular systems 3.2. An algorithm is then given to test if a system admits a block

chained form and to exhibit one 3.3. We then give a sufficient condition for flatness, completed with a condition for regularity, for the various choices of flat outputs 3.4. Sec. 4 is devoted to the simplified aircraft model, which is a flat block diagonal model. The subsection 4.1 is devoted to the various possible choices of flat outputs and their singularities. The outputs x, y, z may be completed with the side-slip angle β 4.1.1, the bank angle μ 4.1.2 or the engines thrust F 4.1.3. Some other possibilities are also mentionned 4.1.4. Stalling conditions and their relations to flatness are investigated 4.2. Section 5 reports simulations using the simplified model, starting with a description of the feed-back design and the Python implementation 5.2. We first consider then initial perturbations 5.3 and the effect of variable wind 5.4. The last section 6 reports experiments with the full model with a Maple implementation 6.1. We start with the F-16C model near stalling conditions 6.2, then gravity free flight 6.3 using flat output μ. The case of a Twin-Otter with a rudder failure is then considered 6.4. A nomenclature is given in appendix A and details on the aircraft models in appendix B.

2 Flatness

For more details on flat systems, we refer to Fliess *et al.* [8, 9] or Lévine [24, 25]. Roughly speaking, the solutions of flat systems are parametrized by m differentially independent functions, called flat outputs, and a finite number of their derivatives. This property, which characterize them, is specialy important for motion planning. We present here flat systems in the framework of diffiety theory [19, 39]. A full understanding of this theoretical setting is not mandatory to understand the more applied sections of the paper.

2.1 Definitions and properties

We will be concerned here with systems of the following shape:

$$x_i' = f_i(x, u, t), \text{ for } 1 \leq i \leq n, \tag{1}$$

where $x_1, \ldots, x_n$ are the state variables and $u_1, \ldots, u_m$ the controls.

In the sequel, we may sometimes denote ∂/∂_x by ∂_x, for short.

Definition 1. *A diffiety is a $\mathcal{C}^\infty$ manifold V of denumerable dimension equipped with a global derivation δ (that is a vector field), the* Cartan derivation *of the diffiety. The ring of functions $\mathcal{O}(V)$ is the ring of $\mathcal{C}^\infty$ function on V depending on a* finite *number of coordinates. The topology on the diffiety is the coarsest topology that makes coordinate functions continuous, i.e. the topology defined by open sets on subspaces of finite dimensions.*

The point 0 *with derivation $\delta := 0$ is considered as a diffiety.*

The trivial diffiety $\mathbf{T}^m$ *is $\left(\mathbb{R}^{\mathbb{N}}\right)^m$ equipped with the derivation $\delta := \sum_{i=1}^m \sum_{k\in\mathbb{N}} z_i^{(k+1)} \partial/\partial_{z_i^{(k+1)}}$.*

The time diffiety $\mathbb{R}_t$ *is $\mathbb{R}$ equipped with the derivation $\delta_t := \partial/\partial t$.*

A morphism of diffiety $\phi : V_1 \mapsto V_2$ is a smooth map between manifolds such that $\phi^* \circ \delta_2 = \delta_1 \circ \phi^*$, where $\phi^* : \mathcal{O}(V_2) \mapsto \mathcal{O}(V_1)$ is the dual application, defined by $\phi^*(f) = f \circ \phi$ for $f \in \mathcal{O}(V_2)$.

A diffiety V is flat if there exists a dense open set $W \subset V$ of flat points*. In that context a point is called flat, if it admits a neighborhood that is diffeomorphic to an open set of $\mathbb{R}_t \times \mathbf{T}^m$. The generators z_i of $\mathbf{T}^m$ are called* linearizing outputs *or* flat outputs. [1]

A set of such flat outputs defines a Lie-Backlünd atlas, as defined in [16].

For a given set of flat outputs, a point is called singular related to this set if it is outside its domain of definition. A point in called an intrinsic singularity if no flat output is defined in a neighborhood of it. Otherwise it is called an apparent singularity.

We illustrate this definition by associating a diffiety to the system considered above.

Example 2. *The product diffiety $\mathbf{T}^m \times \mathbb{R}_t$ is isomorphic to the jet space $\mathbf{J}(\mathbb{R}, \mathbb{R}^m)$. Indeed, points of this jet space can be seen as couples*

$$(t, \sum_{i=1}^m \sum_{k\in\mathbb{N}} \frac{y_i^{(k)}(t)}{k!} \tau^k)$$

[1] Making this high flown terminology more concrete, this means that both the state and input variables x_i, u_i are functions of the z_i and a finite number of their derivatives on one hand. On the other hand, this also means that the z_i are functions of the state and input variables and a finite number of their derivatives, and that the differential dz_i are linearly independent.

and there is a natural action of the derivation d_t *on the ring of function on the jet space* $\mathcal{O}(\mathbf{J}(\mathbb{R},\mathbb{R}^m))$ *that defines a diffiety structure on it. Using* $(t, y_1, y_1', \ldots, y_m, y_m', \ldots)$*, as coordinates, there is a natural bijection* ϕ *between* $\mathbf{T}^m \times \mathbb{R}_t$ *and* $\mathbf{J}(\mathbb{R},\mathbb{R}^m)$*. The derivation* d_t *on the jet space is defined by*

$$\partial_t + \sum_{i=1}^{m}\sum_{k\in\mathbb{N}} u_i^{(k+1)} \frac{\partial}{\partial u_i^{(k)}},$$

so that ϕ *is compatible with the derivations on both diffiety and is a diffiety morphism.*

Example 3. *Any system* (1) *defines a diffiety* $U \times \left(\mathbb{R}^{\mathbb{N}}\right)^m$*, where* $U \subset \mathbb{R}^{n+m+1}$ *is the domain of definition of the functions* f_i*, equipped with the Cartan derivation*

$$\frac{\mathrm{d}}{\mathrm{d}t} := \partial_t + \sum_{i=1}^{n} f_i(x,u,t)\partial_{x_i} + \sum_{j=1}^{m}\sum_{k\in\mathbb{N}} u_j^{(k+1)}\partial_{u_j^{(k)}} \tag{2}$$

Such a system is a normal form *defining the diffiety.*

Flatness may be illustrated by the classical car example.

Example 4. *A very simplified car model is the following:*

$$\left\{\begin{array}{rcl} \dot{x} &=& u\cos\theta \\ \dot{y} &=& u\sin\theta \\ \dot{\theta} &=& \frac{u}{\ell}\tan\varphi \end{array}\right. \tag{3}$$

The state vector is made of the coordinates (x, y) *of the rear axle's center and of the angle* θ *between the car's axis and the x-axis. The controls are the speed* u *and the angle* φ *between the wheels' axis and the car's axis. The length* ℓ *is the distance between the two axles.*

One can define different sets of flat outputs depending on the actual open set, where they are defined, as follows.

1. *Over* $U_1 = \{\dot{x} \neq 0\}$*, we take* $z_{(1)} = (x, y) = \psi_1(\mathfrak{x})$ *and the inverse Lie-Bäcklund transform is given by:*

$$\phi_1 = \begin{pmatrix} x \\ y \\ \tan^{-1}(\frac{\dot{y}}{\dot{x}}) \end{pmatrix}$$

2. *Over* $U_2 = \{\dot{y} \neq 0\}$*, we take* $z_{(2)} = (x, y) = \psi_2(\mathfrak{x})$ *and the inverse Lie-Bäcklund transform is given by:*

$$\phi_2 = \begin{pmatrix} x \\ y \\ \mathrm{cotan}^{-1}(\frac{\dot{x}}{\dot{y}}) \end{pmatrix}$$

3. *Over* $U_3 = \{\dot{\theta} \neq 0\}$*, we take* $z_{(3)} = (\theta, x\sin\theta - y\cos\theta) = \psi_3(\mathfrak{x})$*. Here for the sake of simplicity, we shall denote* (z_1, z_2) *the components of* $z_{(3)}$*. In that case, the inverse Lie-Bäcklund transform is given by:*

$$\phi_3 = \begin{pmatrix} \frac{\dot{z}_2}{\dot{z}_1}\cos z_1 + z_2 \sin z_1 \\ \frac{\dot{z}_2}{\dot{z}_1}\sin z_1 - z_2\cos z_1 \\ z_1 \end{pmatrix}$$

See [16] for all the details.

3 Block diagonal systems

Chained systems are usually considered in the framework of nonholonomic systems and are known to be flat (see *e.g.* Li and Respondek [21] and the references therein). Recently a notion of triangular flat form or generalized chained form has been proposed by Gstöttner *et al.* [12]. We will need first some results related to Jacobi's bound.

3.1 Jacobi's bound

Jacobi's bound was introduced by Jacobi in posthumous manuscripts [32, 33]. It is a bound on the order of a differential system, that is still conjectural in the general case, but was proved by Kondratieva *et al.* [18] under regularity hypotheses in the framework of differential algebra. A presentation using diffiety theory is also available in [34] and one may find complete proofs of the main results of Jacobi in [30], in the setting of differential algebra.

We recall briefly a few basic definitions and properties.

Definition 5. *We denote by S_n the set of bijections from $\{1,\dots,n\}$ to itself.*

Let P_i, $1 \leq i \leq n$ be a differential system in n variables x_j. By convention, if P_i is free of x_j and its derivatives, we define $\operatorname{ord}_{x_j} P_i = -\infty$. *With this convention we define the* order matrix *of P, denoted $A_P := (a_{i,j})$, where $a_{i,j} := \operatorname{ord}_{x_j} P_i$. The* Jacobi number *of the system P is the* tropical determinant *of A_P:*

$$\mathcal{O}_P := \max_{\sigma\in S_n} \sum_{i=1}^{n} a_{i,\sigma(i)}.$$

The tropical determinant may be computed in polynomial time using Jacobi's algorithm [31, 2.2] that relies on the notion of *canon*, that is equivalent to Kuhn's Hungarian method [20] that relies on the notion of *minimal cover*.

Definition 6. *For a $n \times n$ matrix of integers A, a* canon *is a vector of integers $(\ell_1,\dots,\ell_n)$, such that there exists $\sigma_0 \in S_n$ that satisfies, for all $1 \leq j \leq n$, $a_{\sigma_0^{-1}(j),j} + \ell_{\sigma_0^{-1}(j)} = \min_{i=1}^{n} a_{i,j} + \ell_i$. The $a_{i,\sigma(i)}$, for $1 \leq i \leq n$, are a* maximal family of transversal maxima.

It is easily seen that if ℓ is a canon with a maximal family of transversal maxima described by the permutation σ_0, then the tropical determinant of A is $\sum_{i=1}^{n} a_{i,\sigma_0(i)}$.

Definition 7. *A* cover *is a couple of integer vercors μ,ν, such that $a_{i,j} \leq \mu_i + \nu_j$. A* minimal cover *is a cover such that the tropical determinant of A satisfies: $\mathcal{O}_A = \sum_{i=1}^{n}(\mu_i + \nu_i)$.*

To any canon ℓ, one may associate a minimal cover $\mu_i := \max_{\iota=1}^{n} \ell_\iota - \ell_i$ and $\nu_j := \max_{i=1}^{n} a_{i,j} - \mu_i$. See [31, prop. 20]. Using the partial order defined by $\ell \leq \ell'$ if $\ell_i \leq \ell'_i$ for all $1 \leq i \leq n$, there exists a unique minimal canon λ, that satifies $\lambda \leq \ell$ for any canon ℓ. See [31, th. 13] for more details. To this minimal canon, we associate the minimal cover α, β that we call *Jacobi's cover*.

Definition 8. *Let P_i, $1 \leq i \leq n$ be a system in n differential indeterminates $x_1, \dots, x_n$. The* system determinant *or* truncated determinant[2] *is*

$$\nabla_P := \left| \frac{\partial P_i}{\partial x_j^{\alpha_i+\beta_j}} \right|.$$

With this definition, we may state the following result, due to Jacobi.

Theorem 9. *Let P_i, $1 \leq i \leq n$ be a system in n differential indeterminates $x_1, \dots, x_n$ that defines a diffiety V in a neighborhood of a point $\eta \in \mathbf{J}(\mathbb{R},\mathbb{R}^m)$. Then, if ∇_P does not vanish at η, there exist $\sigma \in S_n$ such that the diffiety admits a normal form*

$$x_i^{(\alpha_{\sigma^{-1}(i)}+\beta_i)} = f_i(x),$$

so that the order of the diffiety is $\mathcal{O}_P$.

Proof. See [34, th. 0.3 (ii)]. □

Considering algebraic systems, one may also refer to [31, 6 and 7.1]. The basic idea is to use a new ordering on derivatives, compatible with Jacobi's cover: $\operatorname{ord}^{\mathrm{J}}_{x_j} P := \operatorname{ord}_{x_j} P - \beta_j$. The non vanishing of the system determinant is then precisely the condition required to get a normal formal by applying the implicit function theorem. We illutrate the result with a linear example to make computations easier.

Example 10. *Consider the system $P_1 := x_1 + x_2'$, $P_2 := x_1' - x_2'' + x_3$, $P_3 := x_2''' + x_3'$. We have $\mathcal{O}_P = 3$, $\alpha = (0,1,2)$ and $\beta = (0,1,-1)$. The normal forms compatible with Jacobi's ordering are $x_1 = -x_2'$, $x_2'' = x_3/2$, $x_3' = 0$; $x_1 = -x_2'$, $x_3 = 2x_2$, $x_2''' = 0$; $x_2' = x_1$, $x_1' = -x_3/2$, $x_3' = 0$ and $x_2' = x_1$, $x_3 = 2x_1'$, $x_1'' = 0$.*

[2] Jacobi named it *determinans mancum sive determinans mutilatum* because only the terms $\partial P_i/\partial x_j^{a_{i,j}}$ such that $a_{i,j} = \alpha_i + \beta_j$ appear in it.

3.2 Definition of block triangular systems

Definition 11. *A* block triangular system *is a system of $n-m$ differential equations P_i, in n variables x_j that admits a* block triangular form*, that is a partition $\bigcup_{k=0}^{r}\Xi_k$ of the set of variable and a partition $\bigcup_{k=1}^{r}\Sigma_k$ of the set of equations that satify the five following conditions:*

i) for all $P\in\Sigma_k$, P only depends on variables in $\bigcup_{i=0}^{k}\Xi_i$ and their derivatives;

ii) for all $1\leq k\leq r$ and for all $P\in\Sigma_k$, $\max_{x\in\Xi_k}\mathrm{ord}_x P=0$;

iii) for all $1\leq k\leq r$ and for all $x\in\Xi_k$, $\max_{P\in\Sigma_k}\mathrm{ord}_x P=0$;

iv) for all $1\leq k\leq r$ and for all $x\in\Xi_{k-1}$, $\max_{P\in\Sigma_k}\mathrm{ord}_x P>0$;

v) for all $1\leq k\leq r$, $\sharp\Sigma_k\leq\sharp\Xi_k$ and $\max_{\sigma\in S(\Sigma_k,\Xi_k)}\sum_{P\in\Sigma(k)}\mathrm{ord}_{\sigma(P)}P=0$, where $S(\Sigma_k,\Xi_k)$ denotes the set of injections $\Sigma_k\mapsto\Xi_k$.

Remark 12. *By condition ii), we need have $a_{i,j}=0$ or $a_{i,j}=-\infty$ when $i\in\Sigma_k$ and $j\in\Xi_k$, so that $\sum_{P\in\Sigma(k)}\mathrm{ord}_{\sigma(P)}P=0$ means that $\mathrm{ord}_{\sigma(P)}P=0$ for all $P\in\Sigma_k$. Testing condition iv) is equivalent to the marriage problem and can be tested in $O(n(n-m)^2)$ elementary operations using Jacobi's algorithm or $O(n(n-m)^{3/2})$ elementary operations using Hopcroft and Karp algorithm [31, 3.1].*

We may first remark that a m-chained form [21, def. 2] is a special case of our block diagonal form, as well as the generalized chained forms in Gstöttner *et al.* [12, (6) p. 1146].

Example 13. *A system in m-chained form is represented by:*

$$x'_{0,0}=u_0;\ x'_{i,j}=x_{i,j+1}u_0 \text{ for } 1\leq i\leq m \text{ and } 0\leq j<n;\ x'_{i,n}=u_i \text{ for } 1\leq i\leq m,$$

where m and n are strictly positive integers. It is block triangular with $\Xi_1=\{x_{0,0}\}$, $\Xi_2=\{u_0\}\cup\{x_{i,0}|1\leq i\leq m\}$, $\Xi_{j+2}=\{x_{i,j}|0\leq i\leq m\}$, for $1\leq j\leq n$ and $\Xi_{n+3}=\{u_i|1\leq i\leq m\}$.

Example 14. *A system in generalized chained form is represented by*

$$x'_1=u_2;\ x'_i=x_{i+1}u_2+a_i(x_1,\ldots,x_i) \text{ for } 1\leq i<n; x'_n=u_1,$$

where n is a strictly positive integer. It is block triangular with $\Xi_1=\{x_1\}$, $\Xi_2=\{x_1,u_2\}$, $\Xi_i=\{x_i\}$, for $1<j\leq n$ and $\Xi_{n+1}=\{u_1\}$.

On may remark that, according to our definition, the order of $P\in\Sigma_k$ in $x\in\bigcup_{\kappa=0}^{k-1}\Xi_\kappa$ may be greater that 1 and that the equations P_i can be implicit equations.

Example 15. *The system $P_1:=x_2+x_3-x_1''+x_1$, $P_2:=x_4-x_2'-X_3''+x_2-x_1$ is block diagonal with $\Sigma_i=\{P_i\}$, for $i=1,2$ and $\Xi_0=\{x_1\}$, $\Xi_1=\{x_2,x_3\}$ and $\Xi_2=\{x_4\}$.*

The next theorem is useful to characterize system admiting a block triangular form.

Theorem 16. *i) Assume that P admits a block triangular form with partitions Ξ_k, for $1\leq k\leq r$ and Σ_k, for $0\leq k\leq r$. Then $P\setminus\Sigma_r$ depending on $\{x_1,\ldots,x_n\}\setminus\Xi_r$ admits a block triangular form with partitions Ξ_k, for $1\leq k\leq r-1$ and Σ_k, for $0\leq k\leq r-1$.*

ii) We have $\Xi_r=\{x|\max_{i=1}^{n-m}\mathrm{ord}_x P_i=0\}$ and $\Sigma_r=\{P_i|\max_{x\in\hat{\Xi}_r}\mathrm{ord}_x P_i=0\}$.

iii) The block triangular form is unique.

iv) If a system admits a block triangular form, its order matrix admits a $(n-m)\times(n-m)$ square submatrix with tropical determinant equal to 0.

Proof. Assertion i) is a straightforwars consequence of the definition.

By hypotheses i) and iii) of def. 11, $\Xi_r\subset\{x|\max_{i=1}^{n-m}\mathrm{ord}_x P_i=0\}$; the reverse inclusion is a consequence of hypothesis iv). By hyp. ii), $\Sigma_r\subset\max_{x\in\Xi_r}\mathrm{ord}_x P=0$; the reverse inclusion is a consequence of hyp. i). This proves assertion ii).

Assertion iii) is easilly proved by recurrence on r, using i) and ii).

To prove assertion iv), for all $1\leq k\leq r$, let σ_k be such that $\sum_{P\in\Sigma(k)}\mathrm{ord}_{\sigma_k(P)}P=0$, according to hyp. v). Then, we only have to keep the columns corresponding to state variables in $\bigcup_{i=1}^{k}\mathrm{Im}(\sigma_k)$. □

Remark 17. *Not all systems such that their order matrix contains a square submatrix of tropical determinant* 0 *are block triangular according to our definition. It is enough to add a new variable that does not appear in the equations. This could be taken as an ultimate generalization, but we do not known if this property can be tested in polynomial time.*

In most situations of practical interest, one may expect to consider block triangular systems of order 1 and such that equations in Σ_k are close to normal forms expressing the values of the derivatives of variables in Ξ_{k-1}.

Example 18. *This is the case of the system:* $P_1 := x_1' - x_3^2 + x_4^2$, $P_2 := x_2' - x_4^2 + x_5^2$, $P_3 := x_4' - x_6$, $P_4 := x_5' - x_7$, *for which* $\Xi_0 = \{x_1, x_2\}$, $\Xi_1 = \{x_3, x_4, x_5\}$, $\Xi_3 = \{x_6, x_7\}$ *and* $\Sigma_1 = \{P_1\}$, $\Sigma_2 = \{P_2\}$, $\Sigma_3 = \{P_3, P_4\}$.

3.3 Characterization

In practice, flat systems of small size are mostly considered, and one may easilly check by inspection that a system admits a block triangular form. Anyway, large size systems may also be considered, *e.g.* comming from the discretization of flat PDE's systems [35, 37]. We give an algorithm to test if a system admits a block triangular form. We assume that cond. v) of def. 11 is tested by a routine `HK`.

Algorithm 19. ***Imput:*** *A* $n \times (n-m)$ *matrix* A *with entries* $a_{i,j} \in \mathbb{N} \cup \{-\infty\}$.

$L := \{1, \dots, n\}$; $M := \{1, \dots, n-m\}$; $q := 0$;

until $M = \emptyset$ ***do***

$q := q + 1$; $\Xi_q := \emptyset$; $\Sigma_q := M$;

for $j \in L$ ***do if*** $\max_{i=1}^{n-m} a_{i,j} = 0$ ***then*** $\Xi_q := \{j\} \cup \Xi_q$ ***fi od***;

for $i \in \Sigma_q$ ***do***

for $j \in \Xi_q$ ***do***

if $a_{i,j} > 0$ ***then*** $\Sigma_q := \Sigma_q \setminus \{i\}$ ***fi od od***;

if `HK`$(\Xi_q, \Sigma_q) =$ *"False"* ***then return*** *"Failed"* ***else*** $M := M \setminus \Sigma_q$; $L := L \setminus \Xi_q$ ***fi od***;

$\Xi_{q+1} = L$;

for k ***from*** 1 ***to*** q ***do if*** $P \in \Sigma_k \max_{x \in \Xi_{k-1}} \mathrm{ord}_x P \leq 0$ *or* $x \in \Xi_{k-1} \max_{P \in \Sigma_k} \mathrm{ord}_x P \leq 0$ ***then return*** *"Failed"* ***fi od***;

output: $[\Xi_{q+1}, \dots, \Xi_1]$, $\Sigma_q, \dots, \Sigma_0$.

We remark that the sets Ξ_q and Σ_q are computed in reverse order with respect to the conventions of def. 11, so that Ξ_1 corresponds in fact to Ξ_r after reordering.

Theorem 20. *i) This algorithm returns "Failed" iff the system admits no block triangular form. If it admits one, it returns it.*

ii) Its time complexity is $O(n(n-m)^2)$.

Proof. i) It is easilly proved by recurrence on r, using th. 16 i) and ii).

ii) The number of iterations in each loop is $r \leq n - m$ and the number of elementary operations for each iteration is $O(n(n-m))$. □

The asymptotic complexity of this algorithm may be improved, a topic that is left for further investigations.

3.4 Sufficient flatness conditions

We can now state the main result that shows that generic block triangular systems are flat and exhibit sufficient flatness conditions, related to the possible choices of linearizing outputs.

Theorem 21. *i) If the system* P *locally defines a diffiety* V *as a subdiffiety of the trivial diffiety* $\mathbf{T}^n$ *in a neighborhood of a point* η *and if for all* $1 \leq k \leq r$ *there exists* $Z_k \subset \Xi_k$ *such that*

$$\left| \frac{\partial P}{\partial x} | (x, P) \in Z_k \times \Sigma_k \right| \tag{4}$$

does not vanish, then $\bigcup_{k=0}^{r} Z_k$, *where* $Z_0 = \Xi_0$, *is a regular flat output of* V *at point* η.

ii) With the same hypotheses, if for all $1 \leq k \leq r$, the Jacobian matrix

$$\left(\frac{\partial P}{\partial x}|(x,P) \in \Xi_k \times \Sigma_k\right) \tag{5}$$

has maximal rank at point η, then V is flat at point η.

Proof. i) We first remark that, due to the diagonal structure, the system determinant ∇ can be factored and is equal to

$$\prod_{k=1}^{r} \left|\frac{\partial P}{\partial x}|(x,P) \in Z_k \times \Sigma_k\right|,$$

according to [31, prop. 83]. The assertion is then a straightforward consequence of [34, th. 0.3 ii)]. Please notice, that Jacobi's number is denoted by J in this paper that uses the notion of "diffiety extensions". Any diffiety may be considered as an extension of the diffiety 0 (see def. 1), so all results stand for diffieties as defined here.

ii) We only have to notice that if (5) has full rank, then one may find $Z_k \subset \Xi_k$ such that (4) does not vanish. □

Example 22. *Going back to example 15, we see that it is flat with flat outputs x_1, x_2, x_4 or x_1, x_3, x_4.*

Example 23. *Going back to ex. 18, we see that it is flat when $x_3 x_4 \neq 0$ with flat outputs x_1, x_2, x_5 or when $x_3 x_5 \neq 0$ with flat outputs x_1, x_2, x_4 or when $x_4 x_5 \neq 0$ with flat outputs x_1, x_2, x_3.*

4 The simplified aircraft. A block diagonal system

We study here the model without going into the details of the equations, which are completely described in annex B.

The model is block triangular, with $\Xi_0 := (x, y, z)$, $\Xi_1 := (V, \gamma, \chi)$, $\Xi_2 := (\alpha, \beta, \mu, F)$, $\Xi_3 := (p, q, r)$ and $\Xi_4 := (\delta_\ell, \delta_m, \delta_n)$ or $\Xi_4 := (\delta_\ell, \delta_m, \eta)$ when differential thrust is used. See rem. 25 and B.4 for details.

Example 24. *We can associate a diffiety to our aircraft model, which is defined by $\mathbb{R}^{12} \times \left(\mathbb{R}^{\mathbb{N}}\right)^4$, and a derivation $\eth$ defined by $\eth := \eth_0 + \eth_1$, where $\eth_1$ is the trivial derivation on $\left(\mathbb{R}^{\mathbb{N}}\right)^4$: $\eth_1 := \sum_{z \in \{F, \delta_l, \delta_m, \delta_n\}}^{m} \sum_{k \in \mathbb{N}} z_i^{(k+1)} \partial / \partial z_i^{(k+1)}$ and $\eth_0$ is defined on $\mathbb{R}^{12}$ by the differential equations (21a–21i,22):*

$$\delta_0 := V(t)\cos(\chi(t))\cos(\gamma(t))\frac{\partial}{\partial x} + V(t)\sin(\chi(t))\cos(\gamma(t))\frac{\partial}{\partial y} + \cdots$$

It is flat by prop. 27 in the open set where the Jacobian matrix $\Delta = (\partial Q / \partial \xi | Q \in \{X, \sin(\mu)Y + \cos(\mu)Z, -\cos(\mu)Y + \sin(\mu)Z\};\ \xi \in \Xi_2)$ has full rank (see (27)*), where (X, Y, Z) denotes the forces applied to the aircraft in the wind referential (see (20a–20c)).*

In practice, the diffiety is a smaller open set. The values of the controls are bounded and one wishes to restrict the values of attack angle α or side-slip angle β for safety reasons. The maximal values for the GNA model are given below in table 1. Other limitations must be included, such as the maximal value of the thrust. The speed V should also be greater than the stalling speed (see 4.2).

We will now consider more closely the possible choices of flat outpts.

4.1 Choices of flat outputs

4.1.1 The side-slip angle choice

Martin [26, 27] has used the set of flat outputs: x, y, z, β. We need to explicit under which condition such a flat output may be chosen, *i.e.* when the Jacobian determinant

$$\Delta_\beta = \begin{vmatrix} \frac{\partial X}{\partial \alpha} & \frac{\partial X}{\partial \mu} & \frac{\partial X}{\partial F} \\ \frac{\partial(\sin\mu\, Y + \cos\mu\, Z)}{\partial \alpha} & \frac{\partial(\sin\mu\, Y + \cos\mu\, Z)}{\partial \mu} & \frac{\partial(\sin\mu\, Y + \cos\mu\, Z)}{\partial F} \\ \frac{\partial(\cos\mu\, Y - \sin\mu\, Z)}{\partial \alpha} & \frac{\partial(\cos\mu\, Y - \sin\mu\, Z)}{\partial \mu} & \frac{\partial(\cos\mu\, Y - \sin\mu\, Z)}{\partial F} \end{vmatrix}$$

does not vanish, according to prop. 27. First, we remark, following Martin [26, p. 80] that when $Y = gm\cos(\gamma)\sin(\mu)$ and $Z = gm\sin(\gamma)\sin(\mu)$, *i.e.* when the lift is zero, $\sin\mu\, Y + \cos\mu\, Z = gm\cos(\gamma)$ and $\cos\mu\, Y - \sin\mu\, Z = 0$, so that the last row of D_1 is zero and the determinant vanish. This mean that 0-g flight trajectories are singular for this flat

output. On the other hand, when β and α are close to 0, which is the case in straight and level flight, easy computations using eq. (20a–20c) allow Martin to conclude that

$$|\Delta_\beta| \approx -Z\left(\frac{\rho}{2}SV^2\frac{\partial C_z}{\partial \alpha} + F\right) \gg 0.$$

To go further, one may use the expression of X eq (20a) and deduce from it

$$F = \frac{X + \frac{\rho}{2}SV^2C_x + gm\sin(\gamma)}{\cos(\alpha+\epsilon)\cos(\beta)}, \tag{6}$$

assuming $\cos(\alpha+\epsilon)\cos(\beta)$. Substituting this expression in Y and Z, we define $\tilde{Y}$ and $\tilde{Z}$ and further define $\hat{Y} := \cos(\mu)\tilde{Y} - \sin(\mu)\tilde{Z}$ and $\hat{Z} := \sin(\mu)\tilde{Y} + \cos(\mu)\tilde{Z}$. Then, $|\Delta_\beta| \neq 0$ when

$$\begin{vmatrix} \frac{\partial \hat{Y}}{\partial \alpha} & \frac{\partial \hat{Y}}{\partial \mu} \\ \frac{\partial \hat{Z}}{\partial \alpha} & \frac{\partial \hat{Z}}{\partial \mu} \end{vmatrix} \neq 0. \tag{7}$$

The main interest of this choice is to be able to impose easily $\beta = 0$, which is almost always required.

4.1.2 The bank angle choice

As the angle μ is known, we may compute from Ξ_1' and Ξ_1'' the values X, Y and Z. So, singularities for this flat outputs are such that

$$|\Delta_\mu| = \begin{vmatrix} \frac{\partial X}{\partial \alpha} & \frac{\partial X}{\partial \beta} & \frac{\partial X}{\partial F} \\ \frac{\partial Y}{\partial \alpha} & \frac{\partial Y}{\partial \beta} & \frac{\partial Y}{\partial F} \\ \frac{\partial Z}{\partial \alpha} & \frac{\partial Z}{\partial \beta} & \frac{\partial Z}{\partial F} \end{vmatrix} \neq 0 \tag{8}$$

Using $\tilde{Y}$ and $\tilde{Z}$, as defined in subsec. 4.1.1, we see that this is equivalent to

$$\begin{vmatrix} \frac{\partial \hat{Y}}{\partial \alpha} & \frac{\partial \hat{Y}}{\partial \beta} \\ \frac{\partial \hat{Z}}{\partial \alpha} & \frac{\partial \hat{Z}}{\partial \beta} \end{vmatrix} \neq 0. \tag{9}$$

When β is 0, $\partial\tilde{Z}/\partial\beta$ is also 0, due to the aircraft symmetry. Using the GNA model (see B.3), we have $\partial C_x/\beta = 0$ and $\partial C_z/\partial\beta = 0$, so that $\partial\tilde{Z}/\partial\beta = 0$. The value of the determinant (9) is then

$$-\frac{\partial \hat{Z}}{\partial \alpha}\frac{\partial \hat{Y}}{\partial \beta}. \tag{10}$$

For most aircrafts, $\partial C_y/\partial\beta$ is negative at $\beta = 0$, with values in the range $[-1., -0.5]$. Delta wing aircrafts seem to be a exception, with smaller absolute values (-0.014 for the X-31) or even negative ones ($+0.099$ for the F-16XL). It seems granted that for regular transport planes, $\partial C_y/\partial\beta$ is negative, so that the determinant vanishes only when $\partial\tilde{Z}/\partial\alpha$ is 0. We will see in 4.2 that this may be interpreted as stalling condition and that the vanishing of (10) on a trajectory with constant controls means that the points of this trajectory are flat singularities, so that no other flat outputs could work.

This choice is the best to impose $\mu = 0$ and is natural for decrabe maneuver, that is when landing with a lateral wind, which implies $\beta \neq 0$. We then need to maintain μ close to 0 to avoid the wings hiting the runway.

It is also a good choice when $Y = Z = 0$, a situation that may be encountered in aerobatics or when training for space condition with 0-g flights (see subsec 6.3). The choices β and μ are compared in [30, 7.1] with the simulation of a twin otter flying with one engine.

4.1.3 The thrust choice

The choice of thrust F has one main interest: to set $F = 0$ and consider the case of a aircraft having lost all its engines. The aircraft must land by gliding when all engines are lost. This is a rare situation, but many successful examples are known, including the famous US Airways Flight 1549 [4]. The singularities of this flat output are such that

$$|\Delta_F| = \begin{vmatrix} \frac{\partial X}{\partial \alpha} & \frac{\partial X}{\partial \mu} & \frac{\partial X}{\partial \beta} \\ \frac{\partial(\sin\mu\, Y + \cos\mu\, Z)}{\partial \alpha} & \frac{\partial(\sin\mu\, Y + \cos\mu\, Z)}{\partial \mu} & \frac{\partial(\sin\mu\, Y + \cos\mu\, Z)}{\partial \beta} \\ \frac{\partial(\cos\mu\, Y - \sin\mu\, Z)}{\partial \alpha} & \frac{\partial(\cos\mu\, Y - \sin\mu\, Z)}{\partial \mu} & \frac{\partial(\cos\mu\, Y - \sin\mu\, Z)}{\partial \beta} \end{vmatrix}$$

vanishes. When $F = 0$, by eq. (20a–20c), the vanishing of D_3 is equivalent to

$$\begin{vmatrix} \frac{\partial C_x}{\partial \alpha} & 0 & \frac{\partial C_x}{\partial \beta} \\ \frac{\partial(\cos\mu\, C_z)}{\partial \alpha} & \frac{\partial(\sin\mu\, C_y + \cos\mu\, C_z)}{\partial \mu} & \frac{\partial(\sin\mu\, C_y)}{\partial \beta} \\ \frac{\partial(-\sin\mu\, C_z)}{\partial \alpha} & \frac{\partial(\cos\mu\, C_y - \sin\mu\, C_z)}{\partial \mu} & \frac{\partial(\cos\mu\, C_y)}{\partial \beta} \end{vmatrix} = \frac{\partial C_x}{\partial \alpha}\left(C_y \frac{\partial C_y}{\partial \beta} - C_z \frac{\partial C_x}{\partial \beta}\right).$$

When β vanishes, C_y and $\partial C_z/\partial\beta$ also vanish, due to the aircraft symmetry with respect to the xz-plane. So, we need have $\beta \neq 0$ to use those flat outputs. Using the GNA model, C_x and C_z depend only on α and C_y depends linearly on β.

In the case of a gliding aircraft, situations with $\beta \neq 0$ could precisely be usefull to achieve the forward slip maneuver. When the aircraft is too high, combining non zero β and μ precisely allows a fast descent while keeping a moderate speed. This is very useful when gliding, as there is no option for a go around when approaching the landing strip too high or too fast. This maneuver was performed with success by the "Gimli Glider" [22], Air Canada Flight 143, that ran out of fuel on July 23, 1983, which could land safely in Gimli former Air Force base [22]. A simulation of the forward slip may be found in [30, 7.2].

4.1.4 Other sets of flat outputs

Among the other possible choices for completing the set Ξ_1 in order to get flat outputs, α does not seem to have much specific interest. Indeed,

$$\Delta_\alpha = \begin{vmatrix} \frac{\partial X}{\partial \beta} & \frac{\partial X}{\partial \mu} & \frac{\partial X}{\partial F} \\ \frac{\partial(\sin\mu\, Y + \cos\mu\, Z)}{\partial \beta} & \frac{\partial(\sin\mu\, Y + \cos\mu\, Z)}{\partial \mu} & \frac{\partial(\sin\mu\, Y + \cos\mu\, Z)}{\partial F} \\ \frac{\partial(\cos\mu\, Y - \sin\mu\, Z)}{\partial \beta} & \frac{\partial(\cos\mu\, Y - \sin\mu\, Z)}{\partial \mu} & \frac{\partial(\cos\mu\, Y - \sin\mu\, Z)}{\partial F} \end{vmatrix}$$

Then, $|\Delta_\alpha| = 0$ when

$$\begin{vmatrix} \frac{\partial \hat{Y}}{\partial \beta} & \frac{\partial \hat{Y}}{\partial \mu} \\ \frac{\partial \hat{Z}}{\partial \beta} & \frac{\partial \hat{Z}}{\partial \mu} \end{vmatrix} = 0. \tag{11}$$

Easy computations show that it is the case when $\mu = \beta = 0$, so that α is not a suitable alternative input near stalling conditions.

One may also consider time varying expressions, e.g. linear combinations of β and μ, to smoothly go from one choice to another.

4.2 Stalling conditions

It is known that the lift of a wing reaches a maximum at a critical angle of attack, due to flow separation. This phenomenon can be hardly reversible and create a sudden drop of the lift force Z from its pick value. Our mathematical model is too poor to fully reflect such behavior, but a maximum for the lift can still be computed.

We need to take also in account the contribution of the thrust in the expression of Z, and simple computations show that the critical angle of attack corresponds in our setting to a maximum of $\tilde{Z}$, that is $\partial\tilde{Z}/\partial\alpha = 0$, which corresponds to the singularity for flat output μ already observed above (10).

Three cases may appear with stalling:

1) to reach an extremal value of $\tilde{Z}$, meaning that $\partial\tilde{Z}/\partial\alpha$ vanishes;

2) to reach the maximum thrust $F_{\max}$ before reaching a maximum of $\tilde{Z}$;

3) reaching no maximum of $\tilde{Z}$ with a aircraft with trust/weight ratio greater than 1: in such a case, there is no stalling.

For horizontal straight line trajectories, we may compute the speed V and the thrust F, depending on α, for $\beta = \mu = 0$, using the simplified model. We may also use the full model. As α, β and μ are constants, $p = q = r = 0$, which further allows to express δ_ℓ, δ_m and δ_n depending on α, so that $C_\ell = C_m = C_n = 0$, which is easy with the GNA model that is linear in those quantities.

E.g., For the F4, setting the weight to 38924lb [11], the evaluated stall speed, angle of attack and thrusts are respectively 67.6789m/s (131.56kn), 0.4200rad (24.07°) and 77.0436 for the full model and 64.0904m/s, 0.4366rad and 78.8806

for the simplified one, without thrust limitations. These thrust values are bellow the thrust of J79-GE-17A engines of later versions (79.38kN with afterburning). Assuming a maximal thrust of 2×71.8kN, that corresponds to the J79-GE-2 engines of the first production aircrafts, the stall speed and angle of attack are 67.9835m/s and 0.3969rad with the full model, 64.5515m/s and 0.4057rad with the simplified one. The full model stall speed of about 132kn agrees more or so with the stall speed values of 146KCAS or 148KCAS, according to the models, computed with the NATOPS manual [29, fig. 4.1 and 4.2] at 10000 ft and below and the computed a.o.a of $23°$ with the indicated stall a.o.a of 27 to 28 "units", keeping in mind that those units are not exactly degrees and that our mathematical definition of stalling cannot fully match the actual behaviour. See fig. 1. [2] The case of the F-16C is considered in 6.2.

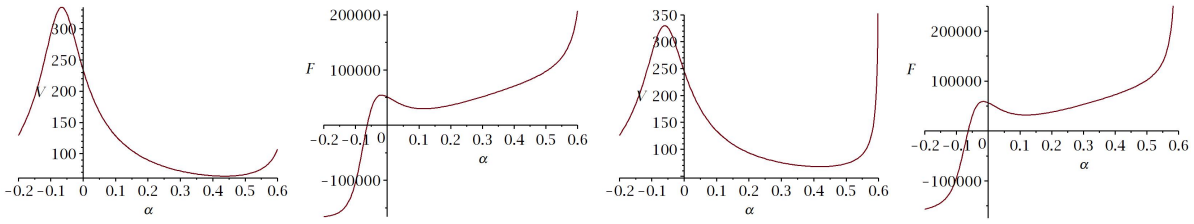

a) b) c) d)

Figure 1: F-4: values of V and F depending on α. a) & b) real model; c) & d) simplified model

5 Simulations using the simplified flat model

In this section, we show simulations done with the flat approximation of the model. These simulations are conducted with the classical set of flat outputs described in section 4.1.1, that is x, y, z, β.

As mentioned above, the flat approximation consists in neglecting the dependency of C_x, C_y, C_z on $p, q, r, \delta_l, \delta_m, \delta_n$. While this approximation, at first sight, may result in some noticeable divergence from the real aircraft, we show here that the model remains robust to various perturbations in the expression of the forces.

This tends to show that in many contexts the flat approximation is quite sufficient.

Moreover, we show that the flat model allows a high flexibility in trajectory planning and tracking.

All these suitable properties remain when one reactor is out of order.

5.1 Theoretical setting for feed-back design

The great advantage of flatness is that the flat motion planning makes an open loop control immediately available. When a closed loop is required, the feedback is designed from the difference between the actual values of the flat outputs and their reference values, so that this difference, being the solution of some differential equation, tends to zero.

In the framework of the flat aircraft model, the feedback is done is two stages. Indeed the dependency of the system variables on F, p, q, r has a slow dynamics in comparison to the rapidity of the dynamics that controls p, q, r from $\delta_l, \delta_m, \delta_n$. This allows to construct a cascade feedback, as done in [27]. More precisely, one can build a dynamic linearizing feedback that allows controlling the partial state vector $\Xi = (x, y, z, V, \alpha, \beta, \gamma, \chi, \mu, F)$ using the command $\dot{F}, p, q, r$, which allows following the reference trajectories of the flat outputs x, y, z, β, using static linearizing feedback. More precisely, one can compute a vector valued function Δ_0 and a matrix valued function Δ_1, both depending on $x, y, z, V, \alpha, \beta, \gamma, \chi, \mu, F$ such that:

$$\begin{pmatrix} x^{(3)} \\ y^{(3)} \\ z^{(3)} \\ \dot{\beta} \end{pmatrix} = \Delta_0 + \Delta_1 \begin{pmatrix} p \\ q \\ r \\ \dot{F} \end{pmatrix}$$

At this stage, the variables $p, q, r, \dot{F}$ are seen as commands. In order to make the system linear, one introduces a new vector valued command v, such that:

$$\begin{pmatrix} p \\ q \\ r \\ \dot{F} \end{pmatrix} = \Delta_1^{-1}(v - \Delta_0)$$

Eventually the command v is chosen of the form:

$$v(t) = \begin{pmatrix} P_0(x_{ref}(t) - x(t)) + P_1(\dot{x}_{ref}(t) - \dot{x}(t)) + P_2(\ddot{x}_{ref}(t) - \ddot{x}(t)) + P_3 x^{(3)}_{ref}(t) \\ P_0(y_{ref}(t) - y(t)) + P_1(\dot{y}_{ref}(t) - \dot{y}(t)) + P_2(\ddot{y}_{ref}(t) - \ddot{y}(t)) + P_3 y^{(3)}_{ref}(t) \\ P_0(z_{ref}(t) - z(t)) + P_1(\dot{z}_{ref}(t) - \dot{z}(t)) + P_2(\ddot{z}_{ref}(t) - \ddot{z}(t)) + P_3 z^{(3)}_{ref}(t) \\ -k_1(\beta_{ref}(t) - \beta(t)) + \dot{\beta}_{ref}(t), \end{pmatrix}$$

where $P(X) = P_0 + P_1 X + P_2 X^2 + P_X^3$ is actually the following polynomial $P(X) = (X - k_1)^3$. Therefore the error function $e_s(t) = s_{ref}(t) - s(t)$ satisfies the following differential equations $P(e_s(t)) = 0$. In our experiments, $k_1 = -5$, so that $e_s(t) \underset{t \to +\infty}{\longrightarrow} 0$, for each value of s in x, y, z, β.

In a second stage the variables p, q, r are controlled through a static linearizing feedback based on $\delta_l, \delta_m, \delta_n$. This part of the system, as mentioned above, is fast in comparison to the first part. More precisely, one can compute the vector valued function Λ_0 and a matrix valued function Λ_1, both depending on $V, \alpha, \beta, p, q, r$ such that:

$$\begin{pmatrix} \dot{p} \\ \dot{q} \\ \dot{r} \end{pmatrix} = \Lambda_0 + \Lambda_1 \begin{pmatrix} \delta_l \\ \delta_m \\ \delta_n \end{pmatrix}$$

Then as previously, one introduced a new command w such that

$$\begin{pmatrix} \delta_l \\ \delta_m \\ \delta_n \end{pmatrix} = \Lambda_1^{-1}(w - \Lambda_0)$$

and

$$w = \begin{pmatrix} -k_2(p_{ref}(t) - p(t)) + \dot{p}_{ref}(t) \\ -k_2(q_{ref}(t) - q(t)) + \dot{q}_{ref}(t) \\ -k_2(r_{ref}(t) - r(t)) + \dot{r}_{ref}(t) \end{pmatrix},$$

where $k_2 = -15$ in our experiments. Therefore $s(t) - s_{ref}(t) \underset{t \to +\infty}{\longrightarrow} 0$, for $s \in \{p, q, r\}$.

The rational behind this cascade feedback is the following. The variables $(x, y, z, V, \alpha, \beta, \gamma, \chi, \mu, F)$ are slowly controlled through $\dot{F}, p, q, r$. Once the required values of p, q, r are known, they are quickly reached through the control performed with $\delta_l, \delta_m, \delta_n$. The respective values of k_1 and k_2 reflect the disparity of speed between the two dynamics.

5.2 Conventions used in our simulations

We now show a series of experiments that illustrate the strength of the flat approximation to control the aircraft in various situations. Those experiments were all performed with GTM extracted from [15]. For the sake of simplicity, we have left the model is imperial units. The implementation is made in Python, relying on the symbolic library `sympy`, the numerical array library `numpy` and the numerical integration of ODE systems from the library `scipy`.

The experiments are all about following a reference trajectory defined by the following expressions:

$$\begin{cases} x_{ref}(t) &= V_1 \cos(\pi(t - Tinitial)/(Tfinal - Tinitial)) \\ y_{ref}(t) &= V_1 \sin(\pi(t - Tinitial)/(Tfinal - Tinitial)) \\ z_{ref}(t) &= -V_2 t - 1000 \\ \beta_{ref}(t) &= 0 \end{cases},$$

where $Tinitial = 0, Tfinal = 30, V_1 = 30, V_2 = 5$. This reference trajectory is an upward helix.

5.3 Initial perturbation

In a second stage, we carried out experiments where the aircraft started away from the reference trajectory and then joined it after a few seconds. If the initial perturbation is not too big, the feedback alone is capable to attract the aircraft to the reference trajectory. If the initial starting point is really far away from the reference trajectory, the flexibility of the flatness based approach allows designing very easily transition trajectory which can be followed with the feedback and that brings to aircraft to the reference upward helix trajectory.

In figure 2, we have rendered the actual trajectory of the aircraft and the flat outputs. It is quite apparent that when the initial perturbation is moderate, the feedback successfully brings the aircraft to the reference trajectory.

The same experiments is performed when a one reactor is broken. Again, we observe that the actual trajectory of the aircraft merges with the reference one, as shown in figure 3. The reference and the actual trajectories merge perfectly, even when starting from a point off the trajectory.

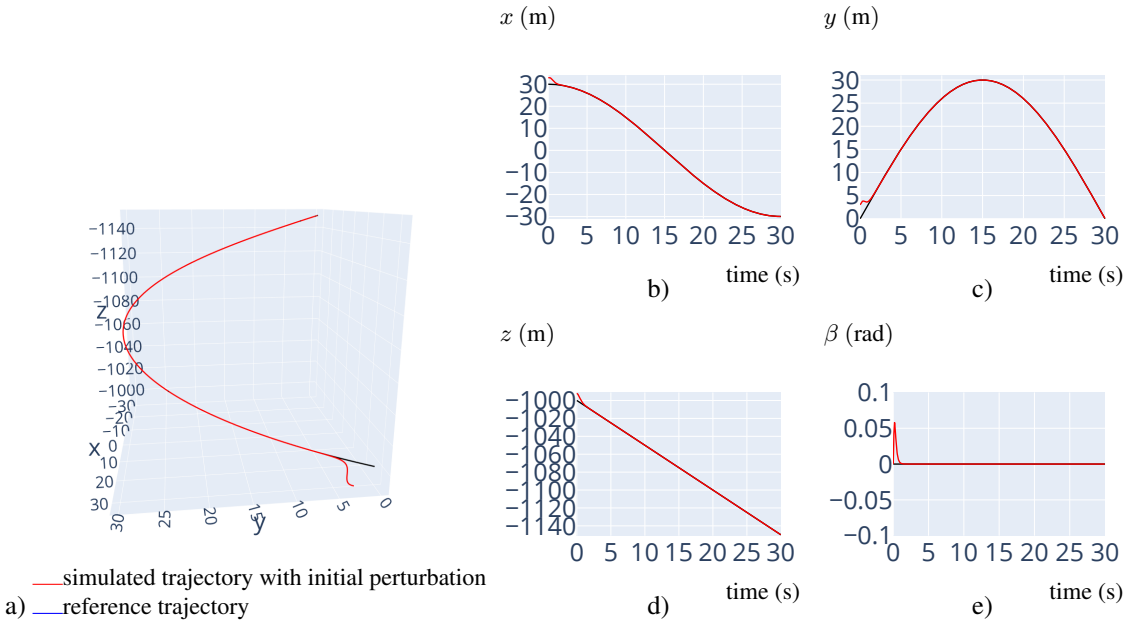

Figure 2: GTM trajectory, starting point aside: the aircraft joins the reference trajectory. a) 3D view; b)–e) Histories of x, y, z, β

.

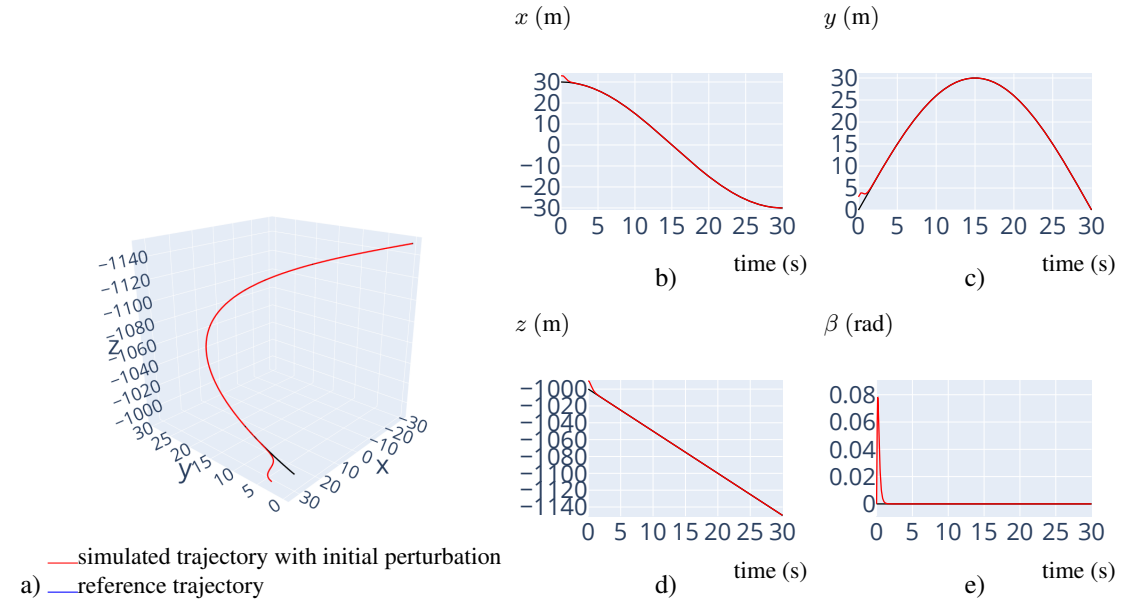

Figure 3: The values of the GTM trajectory, one engine: the aircraft converges toward the reference trajectory. a) Trajectory, 3D view; b)–e) Histories of x, y, z, β

5.4 Variable wind

In this section, we address the most critical problem about the flat approximation. Since the dependency of the aerodynamic coefficient on $p, q, r, \delta_l, \delta_m, \delta_n$ is discarded, one can wonder if the model is robust enough to significant perturbations in the values of the thrust. It turns out that under mild external forces, the model remains reliable.

In the last experiment, the motion of the aircraft is perturbed by a variable wind. This perturbation force is a sinusoidal function which amplitude is 50lbf and frequency is 0.1Hz. This setting is applied to the GTM with the piece-wise trajectory defined above. We observe a very robust behavior of the model, as rendered in figures 4 and 5. The reference and the actual trajectories still merge perfectly with a variable wind. For the variables F, α, p, q, r variations due to the variable wind are noticeable in the graphs.

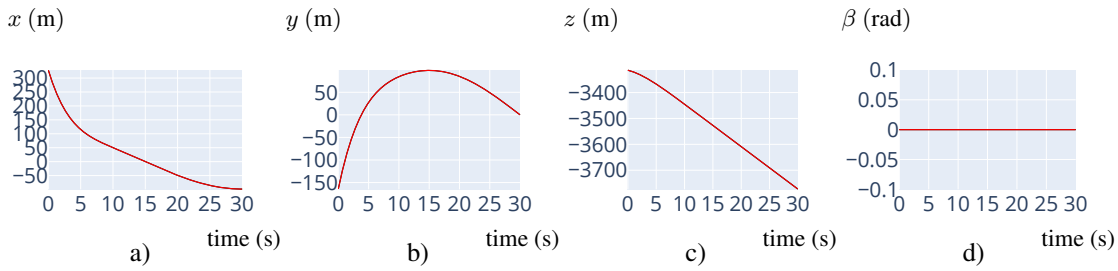

Figure 4: Variable wind. a)–d) Histories of x, y, z, β

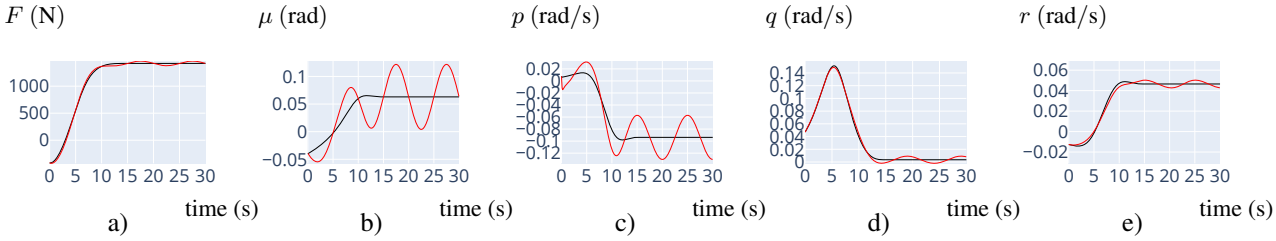

Figure 5: Variable wind. a)–e) Histories of F, μ, p, q, r

6 Simulations using the full model

6.1 Implementation in Maple

Our implementation computes power series approximations of all state variables and control at regular time interval. We proceed in the same way for the feed-back, which is also approximated with power series at the same time interval for better efficiency during numerical integration.

We denote by $\hat{\xi}(t)$ the planed function for any state variable ξ, according to the planification using the simplified flat system and the choice of $\hat{x}$, $\hat{y}$, $\hat{z}$ and $\hat{\beta}$ (or $\hat{\mu}$). We also denote by $\delta\xi$ the difference $\xi - \hat{\xi}$ between the planed trajectory and the trajectory computed with the full model. We did not manage to get a working feed-back without using integrals I_1, I_2, I_3, I_4 of $\cos(\chi)\delta x + \sin(\chi)\delta y$, $-\sin(\chi)\delta x + \cos(\chi)\delta y$, δz and $\delta\beta$ (or $\delta\mu$) respectively. When using the flat outputs x, y, z, F, I_4 is no longer needed.

For the feed-back we choose positive real numbers $\lambda_{i,j}$, with $1 \leq i \leq 4$, and $1 \leq j \leq 5$ for $i = 2$ or $i = 3$ and $1 \leq j \leq 3$ for $i = 1$ or $i = 4$. The value of δF, $\delta\delta_l$, $\delta\delta_m$, $\delta\delta_n$, are computed, so that $\prod_{i=1}^{3}(d/dt + \lambda_{1,i})I_1 = 0$, $\prod_{i=1}^{3}(d/dt + \lambda_{4,i})I_4 = 0$, $\prod_{i=1}^{5}(d/dt + \lambda_{2,i})I_2 = 0$, $\prod_{i=1}^{5}(d/dt + \lambda_{3,i})I_3 = 0$, using the derivation d/dt of the linearized simplified system around the planed trajectory. Then, we use the controls $\hat{\delta}_l + \delta\delta_l$, $\hat{\delta}_m + \delta\delta_m$, $\hat{\delta}_n + \delta\delta_n$, $\hat{F} + \delta F$ in the numerical integration. If the $\delta\xi$ are small enough to behave like the $\mathrm{d}\xi$ of the linearized system, and the solution of the full model not too far from the planed solution of the simplified model, the convergence is granted.

In practice, the choice of suitable $\lambda_{i,j}$ is difficult and empirical: two small, the trajectory is lost, two high, increasing oscillations may appear. We neglect here the dynamics of the actuator, our goal being to show that the feed-back is

able to provide a solution for the full model, using the trajectory planed with the simplified one, the linearizing outputs remaining close to their original values.

Unless otherwise stated, angles are expressed in radians, lengths in meters, times in seconds, thrusts in Newtons, masses in kg. Curves in red correspond to the planed trajectory $\hat{\xi}$, while curves in blue correspond to the integration of the full model. For more clarity z has been replaced by $-z$ to get positive values when drawing curves.

Computation times are real time, not cpu time, using Maple 19 with an Intel processor Core i5 2.5GHz. These are just indications that can vary from a session to an other one.

6.2 High angle of attack with the F16

We consider here with the models of the fighter F-16C linear horizontal trajectories at reduced speed in order to experiment high angle of attack, close to stalling. For both simulations, trajectory tracking is good, with variations for x less than 1m and for z less than 5m.

The F-16 has a thrust to weight ratio greater than 1 with afterburning. The highest thrust engine developped for it, the F110-GE-132, has a maximum thrust of $32,500$lbf (144.6kN), as the weight used in our computations is $20,500$lb. So, the only possibility for stalling is a maximum of $\tilde{Z}$, that occurs with the full model and the simplified one. The computed stall speed, angle of attack and thrust are 43.0408m/s (83.66kn), 0.7656rad ($43.87°$) and 47.8279KN, with the real model, 26.5681m/s, and 1.1957rad and 45.7808KN, with the simplified one. The angle of attack exceeds the limits of the model, but the evaluation with the full model is not so far from the real behaviour. Deep stalls with the F-16 have been reported at about 100kn with an angle of attack arround 50 to $60°$ (Dryden [7]). It corresponds to a loss of control that is difficult to escape and not just a loss of lift. The next fig. 6 provides the computed values of V and F depending on the angle of attack.

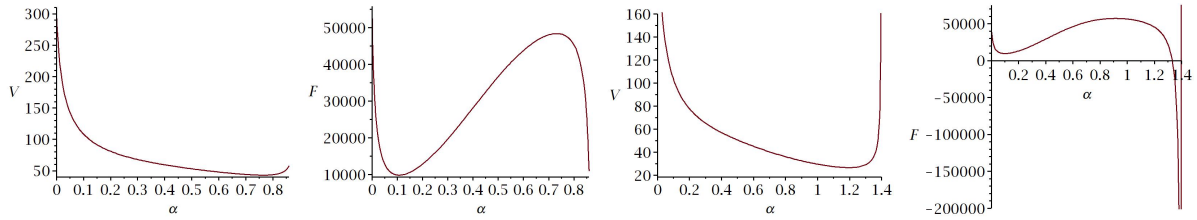

a) b) c) d)

Figure 6: F-16: values of V and F depending on α. a) & b) real model; c) & d) simplified model

The following equations presents the value of the linearizing outputs and $\lambda_{i,j}$ used in the next simulation:

$$\begin{array}{ll} x & = 165t - 125.5\left(\int_0^t \operatorname{atan}\frac{x-60}{10}\mathrm{d}t - \int_0^t \operatorname{atan}\frac{x-120}{10}\mathrm{d}t\right)\mathrm{kn}; \\ y & = 0; \quad z = 0; \quad \mu = 0; \\ \lambda_{i,j} & = 0.5. \end{array} \tag{12}$$

In this simulation, the $\lambda_{i,j}$ are again small by necessity as the feed-back is close to its maximal possibilities. In the planed trajectory, the speed is reduced from 81.6650 at $t = 0$s (actually $V(0.2) = 81.66859$ is the initial maximum during simulation) to reach a minimum 44.48860 at $t = 90$ ($V(90.3 = 44.45203$m/s during simulation), then set back to the initial value ($V(180.) = 81.66516$ during simulation). The minimal speed is quite close to the computed stall speed for the full model: 43.0408m/s. The total computation time for the simulation is 294s. The total computation time for the simulation is 279s. See fig. 7

6.3 Gravity-free flight with the F16

We experiment here a 0-g flight with a parabolic trajectory. Among our models, only the F-16 and the GTM are avaible, for C_z does not vanish with the F4 and the T-O. See fig. 8. For this simulation, we used an expression of air density varying with altitude z, following Martin [26, A.16 p. 97]. The total computation time of the simulation is 371s.

$$\begin{array}{ll} x & = 750t\mathrm{km/h}; \quad y = 0; \quad z = g\frac{t^2}{2} - 2000; \quad \mu = 0; \\ \eta & = 0; \\ \lambda_{i,j} & = 5.; \\ \rho & = 1.225(1 + 0.0065z/288.15)^{(9.80665/287.053\times 0.0065-1)} \end{array} \tag{13}$$

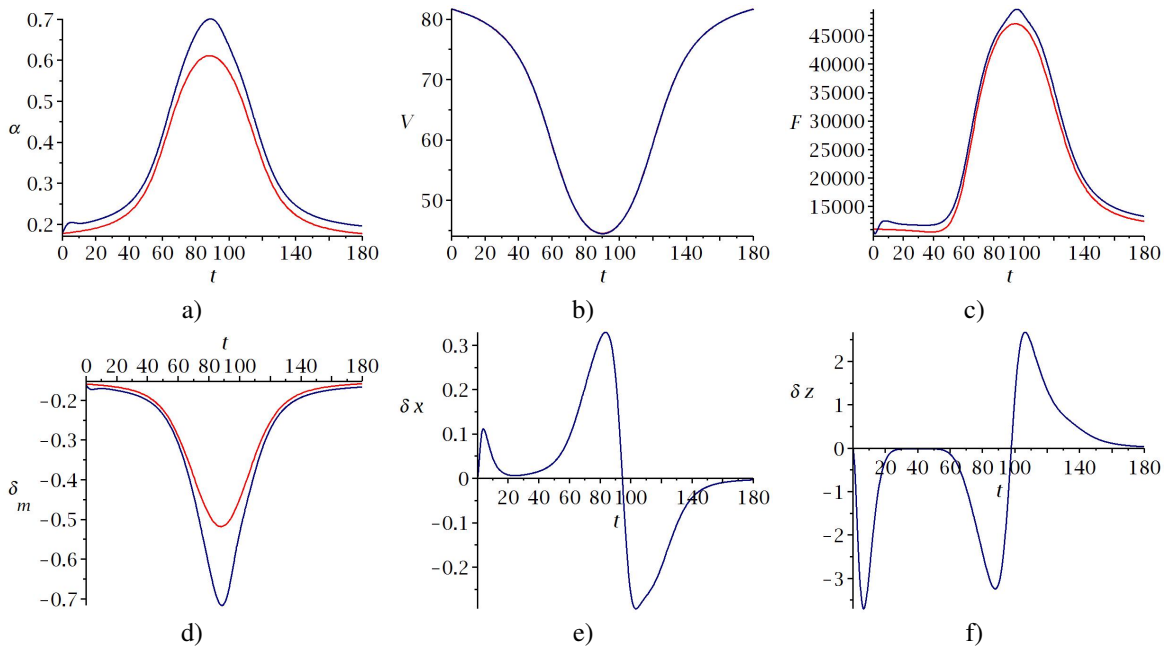

Figure 7: F-16 near stall speed. a) α (rad); b) V (m/s); c) F (N); d) δ_m (rad); e) δx (m) and f) δz (m).

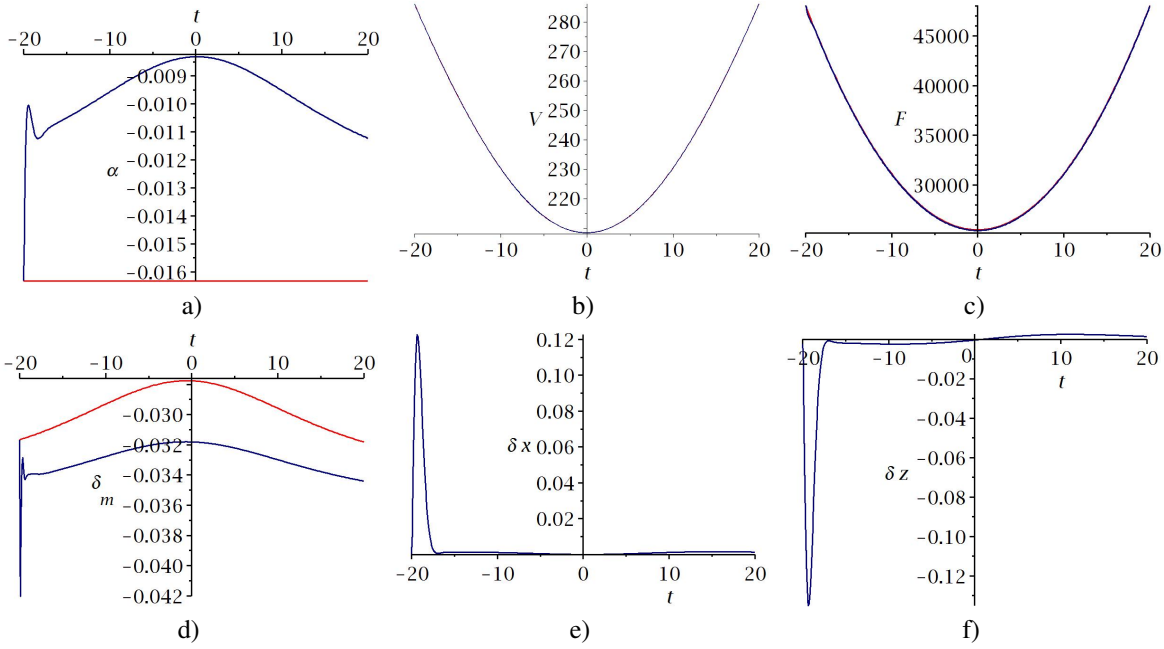

Figure 8: F-16 0-g flight. a) α (rad); b) V (m/s); c) F (N); d) δ_m (rad); e) δx (m) and f) δz (m).

6.4 Rudder failure with the Twin Otter

Rudder failure is a classical situation where differential thrust is known to have been applied with success, which requires that the engines are not used at maximal power during take-off and/or themselves lost. Classical examples include Americal Airlines Flight 96 [3] or 2003 Baghdad DHL attempted shootdown incident [2]. One must notice that in those two cases, the elevators control was lost too, making the attitude control more difficult, an issue that is not addressed here. See also on this topic [5, 6, 14, 23].

We consider here differential thrust control of a T-O with rudder failure. We use flat outputs with β, and η is the control that replaces δ_n, set to $20°$. This constant value is taken in account in the simplified model. We use a descending near circular trajectory with speed close to 80kn.

$$\begin{array}{ll} x & = 1100\cos(\frac{80\text{kn}}{1100}t); \\ y = & 1200\sin(\frac{80\text{kn}}{1100}t); \\ z = & 5.5\text{ft}t + 0.025\text{ft}t^2 - 500; \\ \beta & = 0; \\ \lambda_{i,j} & = 5.5 \end{array} \tag{14}$$

The value of δ_n is set to $20°$ and η is used as a new control in order to simulate differential thrust control of the aircraft. The constant value of δ_n is used in the expression of C_x, C_y and C_z for the simplified model, only δ_l and δ_n being set to 0. The strong action of the controls during this circular trajectory implies a rather high value for all the $\lambda_{i,j}$. Precision is good, less to 2.2cm for δz and much less after oscillations during the first 10s of simultion. Nethertheless, small oscillations never stop for q and some other state functions. The T-O is the model for which designing a suitable feed-back is the most difficult. The maximal power for a single engine during the simulation is 537.4hp, bellow the maximal power 550shp (410 kW) of the Pratt & Whitney PT6A-20 engines of the T-O series 1, 100 and 200; the 300 series was fitted with PT6A-27 engines of 680hp (510kW), flat-rated to 620hp (460kW). The total computation time is 3500s. See fig. 9. One may notice the variations of μ and the control δ_m, due to the thrusts neglected in the simplified model.

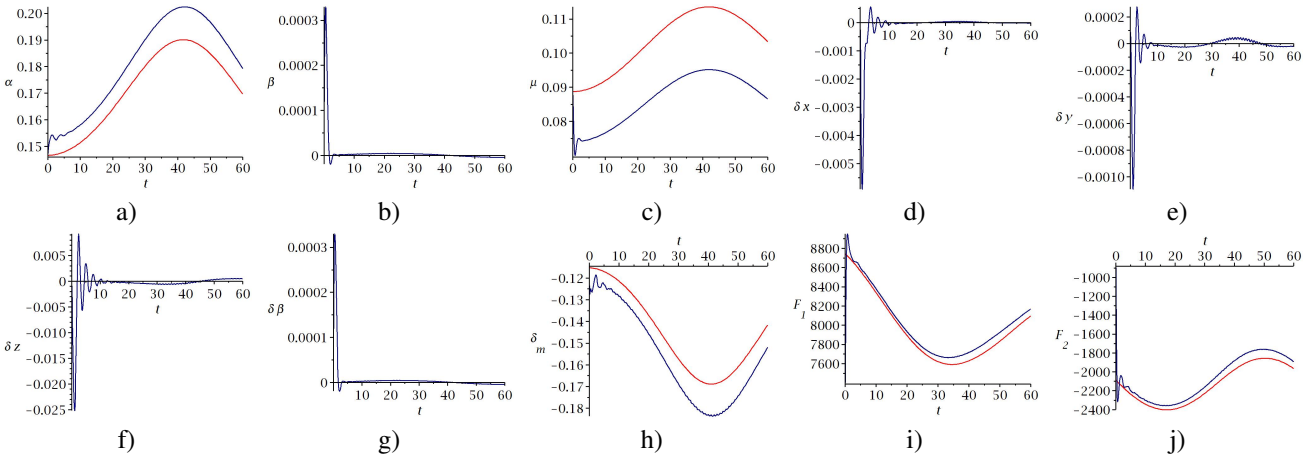

Figure 9: T-O rudder failure flight. a) α (rad); b) β (rad); c) μ (rad); d) δx (m); e) δy (m); f) δz (m); g) $\delta\beta$ (rad); h) δ_m (rad); i) F_1 (N) and j) F_2 (N).

7 Conclusion

We have seen that flat control could be used with some reliability, even in some situations where the validity of the required simplifications in the equations can be questionned, and in various failure conditions.

This research shows how a non-flat system can be controlled by a suitable feedback along a trajectory designed for a flat approximation. This raises numerous theoretical questions concerning the convergence of such a procedure in a general setting and the meaning and interpretation of the limit trajectory, that have been sketched in [30] and will be addressed in future works.

A Nomenclature

Roman

a: wing span

C_x, C_y, C_z: aerodynamic force coefficients, wind frame

C_D, C_L: lift and drag coefficient in aircraft frame

C_l, C_m, C_n: aerodynamic moment coefficients

c: mean aerodynamic chord

F: thrust

L, M, N: aerodynamic moments

m: mass
p, q, r: roll, pitch and yaw rates
S: wing area
V: airspeed
X, Y, Z: aerodynamic forces
y_p: distance of the engines to the plane of symmetry
Greek
α angle of attack
β sideslip angle
γ: flight path angle
η: differential thrust ratio
ϑ: pitch angle
θ: parameters
μ: bank angle
ϕ: roll angle
χ: aerodynamic azimuth or heading angle
ψ: yaw angle
δ_l, δ_m, δ_n: aileron, elevator, rudder deflexion
θ: model parameters

B Aircraft Model

The model presented here relies on Martin [26, 27]. On may also refer to Asselin [1], Gudmundsson [13] or McLean [28] for more details.

B.1 Earth frame, wind frame and body frame

We use an earth frame with origin at ground level, with z-axis pointing downward, as in the figure 10 (left). The coordinates of the gravity center of the aircraft are given in this referential.

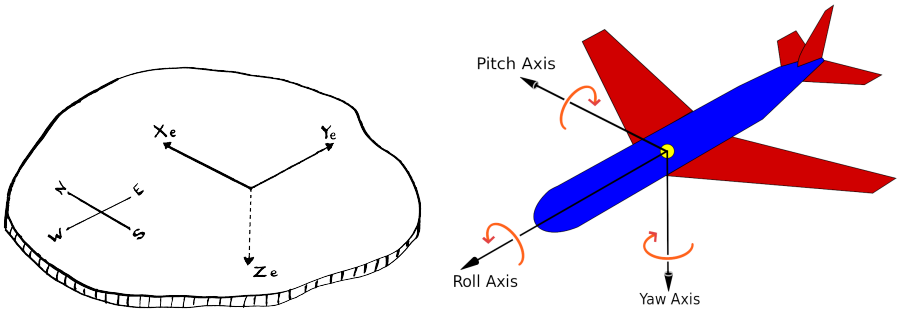

a) b)

Figure 10: a) Earth frame and b) body frame.

The body frame or aircraft referential is defined as in figure 10 (right), where x_b corresponds to the roll axis, y_b to the pitch axes and z_b to the yaw axes, oriented downward. The angular velocity vector (p, q, r) is given in this referential, or to be more precise, at each time, in the Galilean referential that is tangent to this referential.

We go from earth referential to body referential using first a rotation with respect to z axis by the yaw angle ψ, then a rotation with respect to y axis by the pitch angle ϑ, and last a rotation with respect to x axis by the roll angle ϕ, which gives a rotation matrix:

$$R_{eb} = \begin{bmatrix} \cos(\psi(t))\cos(\vartheta(t)) & \sin(\phi(t))\sin(\vartheta(t))\cos(\psi(t)) - \sin(\psi(t))\cos(\phi(t)) & \sin(\phi(t))\sin(\psi(t)) + \sin(\vartheta(t))\cos(\phi(t))\cos(\psi(t)) \\ \sin(\psi(t))\cos(\vartheta(t)) & \sin(\phi(t))\sin(\psi(t))\sin(\vartheta(t)) + \cos(\phi(t))\cos(\psi(t)) & -\sin(\phi(t))\cos(\psi(t)) + \sin(\psi(t))\sin(\vartheta(t))\cos(\phi(t)) \\ -\sin(\vartheta(t)) & \sin(\phi(t))\cos(\vartheta(t)) & \cos(\phi(t))\cos(\vartheta(t)) \end{bmatrix}. \tag{15}$$

The wind frame, with origin the center of gravity of the aircraft has an axis x_w, in the direction of the velocity of the aircraft, the axis z_w being in the plane of symmetry of the aircraft. The Euler angles that define the orientation of the wind frame in the earth frame are denoted $\chi(t), \gamma(t), \mu(t)$, and are respectively the *aerodynamic azimuth* or *heading angle*, the *flight path angle* and the *aerodynamic bank angle*, positive if the port side of the aircraft is higher than the starboard side. See figure 11 (left). We go from earth referential to wind referential using first a rotation with respect to z axis by the *heading angle* χ, then a rotation with respect to y axis by the *flight path angle* γ, and last a rotation with

respect to x axis by the *bank angle* μ, which gives a rotation matrix:

$$R_{ew} = \begin{bmatrix} \cos(\chi(t))\cos(\gamma(t)) & \sin(\mu(t))\sin(\gamma(t))\cos(\chi(t)) - \sin(\chi(t))\cos(\mu(t)) & \sin(\mu(t))\sin(\chi(t)) + \sin(\gamma(t))\cos(\mu(t))\cos(\chi(t)) \\ \sin(\chi(t))\cos(\gamma(t)) & \sin(\mu(t))\sin(\chi(t))\sin(\gamma(t)) + \cos(\mu(t))\cos(\chi(t)) & -\sin(\mu(t))\cos(\chi(t)) + \sin(\chi(t))\sin(\gamma(t))\cos(\mu(t)) \\ -\sin(\gamma(t)) & \sin(\mu(t))\cos(\gamma(t)) & \cos(\mu(t))\cos(\gamma(t)) \end{bmatrix}. \tag{16}$$

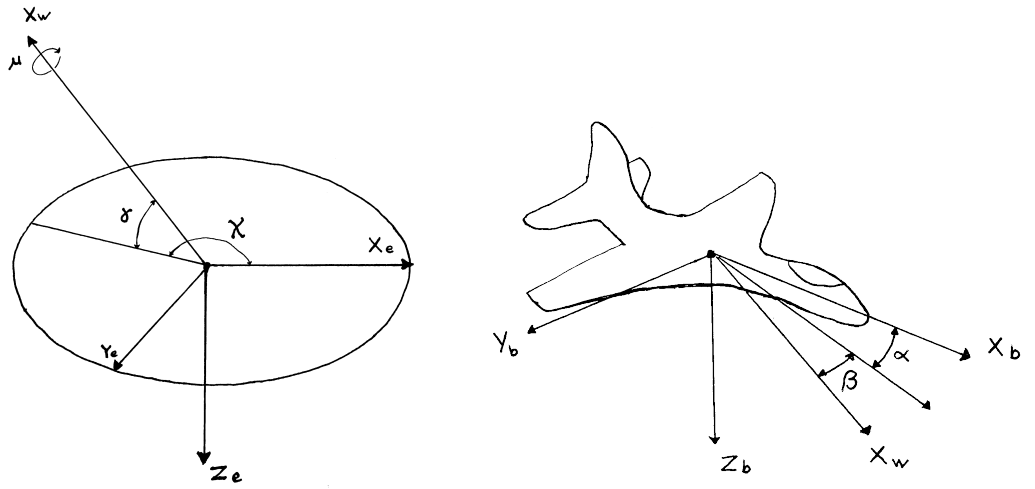

a) b)

Figure 11: a) Wind frame and b) From wind to body frame.

The orientation of the wind frame with respect to the body frame is defined by two angles: the *angle of attack* $\alpha(t)$ and the *sideslip angle* $\beta(t)$, which is positive when the wind is on the starboard side of the aircraft, as in figure 11 (right). We go from the wind referential to the body referential using first a rotation with respect to z axis by the side slip angle β and then a rotation with respect to y axis by the angle of attack α, which gives a rotation matrix:

$$R_{wb} = \begin{bmatrix} \cos(\alpha(t))\cos(\beta(t)) & \sin(\beta(t)) & \sin(\alpha(t))\cos(\beta(t)) \\ -\sin(\beta(t))\cos(\alpha(t)) & \cos(\beta(t)) & -\sin(\alpha(t))\sin(\beta(t)) \\ -\sin(\alpha(t)) & 0 & \cos(\alpha(t)) \end{bmatrix}. \tag{17}$$

B.2 Dynamics

In the sequel, we shall write $p(t), q(t), r(t)$ the coordinates of the rotation vector of the body frame with respect to the the earth frame expressed in the Galilean referential that coincide at time t with the body frame, and $L(t)$, $M(t)$, $N(t)$ the corresponding torques. In the same way $X(t)$, $Y(t)$ and $Z(t)$ denote the forces applied on the aircraft, expressed in the Galilean referential that coincide at time t with the the wind referential.

B.2.1 Aircraft geometry

The mass of the aircraft is denoted by m, S is the surface of the wings. In the body frame, we assume that the aircraft is symmetrical with respect to the xz-plane, so that the tensor of inertia has the following form:

$$J := \begin{bmatrix} I_{xx} & 0 & -I_{xz} \\ 0 & I_{yy} & 0 \\ -I_{xz} & 0 & I_{zz} \end{bmatrix}. \tag{18}$$

In the standard equations (23), we also need a, that stands for the *wing span* and b for the *mean aerodynamic chord*.

B.2.2 Forces and torques

The forces and torques exerted on the aircraft can be easily enumerated:

1. Propulsion force F and torque T_p, which is the sum of the propulsion force and torque of each reactor: $F = F_1 + F_2$ and T_p proportional to $y_p(F_1 - F_2)$, where y_p is the distance of the engines to the plane of symmetry;

2. Aerodynamic force and torque

$$F_a = \rho/2SV^2C_f, \text{ with } C_f = (C_x, C_y, C_z)^{\mathrm{t}} \tag{19a}$$
$$T_a = \rho/2SV^2C_t, \text{ with } C_t = (C_\ell, C_m, C_n)^{\mathrm{t}} \tag{19b}$$

   where ρ is the volumetric mass of air;

3. Weight: gm, which gives no torque.

The force (X, Y, Z) in the wind frame and the torque (L, M, N) are then expressed by the next formulas:

$$X = F(t)\cos(\alpha+\epsilon)\cos(\beta(t)) - \frac{\rho}{2}SV(t)^2C_x - gm\sin(\gamma(t)); \tag{20a}$$
$$Y = F(t)\cos(\alpha+\epsilon)\sin(\beta(t)) + \frac{\rho}{2}SV(t)^2C_y + gm\cos(\gamma(t))\sin(\mu(t)); \tag{20b}$$
$$Z = -F\sin(\alpha+\epsilon) - \frac{\rho}{2}SV(t)^2C_z + gm\cos(\gamma(t))\cos(\mu(t)); \tag{20c}$$
$$L = -y_p\sin(\epsilon)(F_1(t) - F_2(t)) + \frac{\rho}{2}SV(t)^2aC_l; \tag{20d}$$
$$M = \frac{\rho}{2}SV(t)^2bC_m; \tag{20e}$$
$$N = y_p\cos(\epsilon)(F_1(t) - F_2(t)) + \frac{\rho}{2}SV(t)^2aC_n. \tag{20f}$$

The angle ϵ is related to the lack of parallelism of the reactors with respect to the $xy-$plane in the body frame and is small. In the last expressions, we leave the terms depending on ϕ and ϑ for simplicity, but in our computations they are replaced by their expressions depending on γ, μ, α and β, using $R_{eb} = R_{wb}R_{ew}$.

The aerodynamic coefficients $C_x, C_y, C_z, C_l, C_m, C_n$ depend on α and β and also on the angular speeds p, q, r and the controls are virtual angles δ_l, δ_m and δ_n, that respectively express the positions of the ailerons, elevator and rudder.

Remark 25. *One may use $\eta = (F_1 - F_2)/(F_1 + F_2)$ as an alternative control instead of δ_n in case of rudder jam.*

B.2.3 Equations

Following Martin [26, 27], the dynamics of the system is modeled by the following set of explicit differential equations (21a–21i,22):

$$\frac{d}{dt}x(t) = V(t)\cos(\chi(t))\cos(\gamma(t)); \tag{21a}$$

$$\frac{d}{dt}y(t) = V(t)\sin(\chi(t))\cos(\gamma(t)); \tag{21b}$$

$$\frac{d}{dt}z(t) = -V(t)\sin(\gamma(t)); \tag{21c}$$

$$\frac{d}{dt}V(t) = \frac{X}{m}; \tag{21d}$$

$$\frac{d}{dt}\gamma(t) = -\frac{Y\sin(\mu(t)) + Z\cos(\mu(t))}{mV(t)}; \tag{21e}$$

$$\frac{d}{dt}\chi(t) = \frac{Y\cos(\mu(t)) - Z\sin(\mu(t))}{\cos(\gamma(t))mV(t)}; \tag{21f}$$

$$\frac{d}{dt}\alpha(t) = \frac{1}{\cos(\beta(t))}(-p\cos(\alpha(t))sin(\beta(t)) + q\cos(\beta(t)) - r\sin(\alpha(t))\sin(\beta(t)) + \frac{Z}{mV(t)}); \tag{21g}$$

$$\frac{d}{dt}\beta(t) = +p\sin(\alpha(t)) - r\cos(\alpha(t)) + \frac{Y}{mV(t)}; \tag{21h}$$

$$\begin{aligned}\frac{d}{dt}\mu(t) = \ & \tfrac{1}{\cos(\beta(t))}(p\cos(\alpha(t)) + r\sin(\alpha(t)) \\ & + \tfrac{1}{mV(t)}(Y\cos(\mu(t))\tan(\gamma(t))\cos(\beta(t)) - Z(\sin(\mu(t))\tan(\gamma(t))\cos(\beta(t)) + sin(\beta(t)))));\end{aligned} \tag{21i}$$

$$\begin{pmatrix} \frac{d}{dt}p(t) \\ \frac{d}{dt}q(t) \\ \frac{d}{dt}r(t) \end{pmatrix} = J^{-1}\begin{pmatrix} (I_{yy} - I_{zz})qr + I_{xz}pq + L \\ (I_{zz} - I_{xx})pr + I_{xz}(r^2 - p^2) + M \\ (I_{xx} - I_{yy})pq - I_{xz}rq + N \end{pmatrix}. \tag{22}$$

We recall that in the last expressions, the terms depending on gravity do not appear as in Martin [26], but have been incorporated to the expressions X, Y and Z, as in [27].

We notice with Martin that this set of equations imply $\cos(\beta)\cos(\gamma)V \neq 0$. The non vanishing of V and $\cos(\beta)$ seems granted in most situations; the vanishing of V may occur with aircrafts equipped with vectorial thrust, which means a larger set of controls, that we won't consider here. The vanishing of $\cos(\gamma)$ can occur with loopings etc. and would require the choice of a second chart with other sets of Euler angles.

B.3 The GNA model

In the last equations, ρ can depend on z, as the air density vary with altitude. The expression of C_x and C_z could also depend on z to take in account ground effect. These expressions that depend on α, β, p, q, r, δ_l, δ_m and δ_n, should also depend on the Mach number, but most available formulas are given for a limited speed range and the dependency on V is limited to the V^2 term in factor. In the literature, the available expressions are often partial or limited to linear approximations. McLean [28] provides such data for various types of aircrafts; for different speed and flight conditions, including landing conditions with gears and flaps extended.

We have chosen here to use the Generic Nonlinear Aerodynamic (GNA) subsonic models, given by Grauer and Morelli [11] that cover a wider range of values, given in the following table. Among the 8 aircrafts in their database, we have made simulations with 4: fighters F-4 and F-16C, STOL utility aircraft DHC-6 Twin Otter and the sub-scale model of a transport aircraft GTM (see [15]).

$-4^\circ \leq \alpha \leq 30^\circ$	$-20^\circ \leq \beta \leq 20^\circ$,	
$-100^\circ/\text{s} \leq p \leq 100^\circ/\text{s}$	$-50^\circ/\text{s} \leq q \leq 50^\circ/\text{s}$	$-50^\circ/\text{s} \leq r \leq 50^\circ/\text{s}$
$-10^\circ \leq \delta_l \leq 10^\circ$	$-20^\circ \leq \delta_m \leq 10^\circ$	$-30^\circ \leq \delta_n \leq 30^\circ$

Table 1: Range of values for the GNA model

The GNA model depends on 45 coefficients:

$$\begin{array}{rcl} C_D &=& \theta_1 + \theta_2\alpha + \theta_3\alpha\tilde{q} + \theta_4\alpha\delta_m + \theta_5\alpha^2 + \theta_6\alpha^2\tilde{q} + \theta_7\delta_m + \theta_8\alpha^3 + \theta_9\alpha^3\tilde{q} + \theta_{10}\alpha^4, \\ C_y &=& \theta_{11}\beta + \theta_{12}\tilde{p} + \theta_{13}\tilde{r} + \theta_{14}\delta_l + \theta_{15}\delta_n, \\ C_L &=& \theta_{16} + \theta_{17}\alpha + \theta_{18}\tilde{q} + \theta_{19}\delta_n + \theta_{20}\alpha\tilde{q} + \theta_{21}\alpha^2 + \theta_{22}\alpha^3 + \theta_{23}\alpha^4, \\ C_l &=& \theta_{24}\beta + \theta_{25}\tilde{p} + \theta_{26}\tilde{r} + \theta_{27}\delta_l + \theta_{28}\delta_n \\ C_m &=& \theta_{29} + \theta_{30}\alpha + \theta_{31}\tilde{q} + \theta_{32}\delta_e + \theta_{33}\alpha\tilde{q} + \theta_{34}\alpha^2\tilde{q} + \theta_{35}\alpha^2\delta_e + \theta_{36}\alpha^3\tilde{q} + \theta_{37}\alpha^3\delta_e + \theta_{38}\alpha^4, \\ C_n &=& \theta_{39}\beta + \theta_{40}\tilde{p} + \theta_{41}\tilde{r} + \theta_{42}\delta_l + \theta_{43}\delta_n + \theta_{44}\beta^2 + \theta_{45}\beta^3, \end{array} \tag{23}$$

where $\tilde{p} = ap$, $\tilde{r} = ar$, $\tilde{q} = bq$ (see B.2.1 for the meaning of a and b), C_D and C_L correspond to the lift and drag coefficients in the aircraft frame. The coefficients C_x and C_z in the wind frame are then obtained by the formulas:

$$\begin{array}{rcl} C_x &=& \cos(\alpha)C_D + \sin(\alpha)C_L, \\ C_z &=& \cos(\alpha)C_L - \sin(\alpha)C_D. \end{array} \tag{24}$$

Definition 26. *The simplified model is obtained by replacing p, q, r, δ_ℓ, δ_m an δ_n by 0 (or some known constants) in the expressons of C_x, C_y and C_z.*

B.4 Block triangular structure of the simplified model

Using the simplified model, with $\Xi_0 := (x, y, z)$, $\Xi_1 := (V, \gamma, \chi)$, $\Xi_2 := (\alpha, \beta, \mu, F)$, $\Xi_3 := (p, q, r)$ and $\Xi_4 := (\delta_\ell, \delta_m, \delta_n)$ or $\Xi_4 := (\delta_\ell, \delta_m, \eta)$ when differential thrust is used (see rem. 25), we see that, for $1 \leq k \leq 3$, $\dot{\Xi}_i$ only depends on $\bigcup_{\kappa=0}^{k+1} \Xi_\kappa$, so that the model is block diagonal with Σ_1 corresponding to (21a–21c), Σ_2 corresponding to (21d–21f), Σ_3 corresponding to (21g–21i) and Σ_4 to (22).

Simple computations show that

$$\left|\frac{\partial P}{\partial \xi}|P \in \Sigma_1;\ \xi \in \Xi_1\right| = -V^2\cos(\gamma); \quad \left|\frac{\partial P}{\partial \xi}|P \in \Sigma_3;\ \xi \in \Xi_3\right| = \frac{1}{\cos}(\beta), \tag{25}$$

That do not vanish. In the same way,

$$\left|\frac{\partial P}{\partial \xi}|P \in \Sigma_4;\ \xi \in \Xi_3\right| = \frac{\rho^3}{8}S^3V^6a^2b|J|^{-1}\left|\frac{\partial C_i}{\partial \delta_j}|(i,j) \in \{\ell, m, n\}^2\right|, \tag{26}$$

does not vanish as the diagonal terms $\partial C_i/\partial\delta_i$, $i = \ell, m, n$, are much bigger than the others.

So, to apply th. 21, we only need to consider the rank of the Jacobian matrix

$$\left(\frac{\partial P}{\partial \xi}|P \in \Sigma_2;\ \xi \in \Xi_2\right),$$

which is equal to the rank of the Jacobian matrix

$$\Delta := \left(\frac{\partial Q}{\partial \xi}|Q \in \{X, \sin(\mu)Y + \cos(\mu)Z, -\cos(\mu)Y + \sin(\mu)Z\};\ \xi \in \Xi_2\right). \tag{27}$$

Proposition 27. *The simplified aircraft is flat when the matrix Δ has full rank.*

Let $Delta_\xi$ be the matrix Δ where the column corresponding to $\xi \in \Xi_2$ has been suppressed. If $|\Delta_\xi| \neq 0$ at some point, then x, y, z, ξ is a regular flat output at that point.

Proof. This is a direct consequence of th. 21 ii). □

References

[1] Mario Asselin, *An introduction to aircraft performance*, American Institute of Aeronautics and Astronautics, 1997.

[2] Civil Aviation Safety Authority, *The flight crew of an A300 hit by a missile shortly after take-off manage to turn their aircraft around and put it down safely*, Flight Safety Australia (2004).

[3] National Transportation Safety Board, *Aircraft accident report NTSB/AAR-73-02: American Airlines, Inc. McDonnell Douglas DC-10-10, N103AA. Near Windsor, Ontario, Canada. 12 June 1972*, 1973.

[4] _____, *Loss of thrust in both engines after encountering a flock of birds and subsequent ditching on the Hudson River US Airways Flight 1549 Airbus A320-214, N106US Weehawken, New Jersey January 15, 2009*, 2010.

[5] Frank Burcham, Jr., John Burken, Trindel Maine, and John Bull, *Emergency flight control using only engine thrust and lateral center-of-gravity offset: A first look*, Proc. of the 33rd Joint Propulsion Conference and Exhibit (Reston, VA), AIAA, 1997, pp. 207–216.

[6] Frank Burcham, Jr., Trindel Maine, John Burken, and John Bull, *Engine thrust for emergency flight control: MD-11 and B-747 results*, Technical Memorandum 206552, NASA, Dryden Flight Research Center, 1998.

[7] Joe Bill Dryden, *Recovering from deep stalls and departures*, Code One (1987).

[8] Michel Fliess, Jean Lévine, Philippe Martin, and Pierre Rouchon, *Flatness and defect of non-linear systems: introduction theory and examples*, Int. Journal of Control **61** (1995), no. 6, 1327–1361.

[9] _____, *A lie-bäcklund approach to equivalence and flatness of nonlinear systems*, IEEE Trans. Automatic Control **44** (1999), no. 5, 922–937.

[10] Jaume Franch, Sunil Agrawal, S. Oh, and Abbas Fattah, *Design of differentially flat planar space robots: a step forward in their planning and control*, vol. 4, 11 2003, pp. 3053 – 3058 vol.3.

[11] Jared A. Grauer and Eugene A. Morelli, *A generic nonlinear aerodynamic model for aircraft*, AIAA Atmospheric Flight Mechanics Conference, 2014.

[12] Conrad Gstöttner, Bernd Kolar, and Markus Schöberl, *A structurally flat triangular form based on the extended chained form*, International Journal of Control **95** (2022), no. 5, 1144–1163.

[13] Snorri Gudmundsson, *General aviation aircraft design: applied methods and procedures*, Butterworth-Heinemann (Elsevier), Oxford, 2014.

[14] Muhammad Abdul Hannan, Shaoping Wang, and Xingjian Wang, *Fault tolerant control based on differential engine thrust and ailerons of a damaged aircraft with vertical tail loss*, 14th International Bhurban Conference on Applied Sciences and Technology (IBCAST), 2017, pp. 305–311.

[15] R.M. Hueschen, *Development of the transport class model (tcm) aircraft simulation from a sub-scale generic transport model (gtm) simulation*, Technical Memorandum 217169, NASA, Langley Research Center, Hampton, VA, 2011.

[16] Yirmeyahu Kaminski, Jean Lévine, and François Ollivier, *Intrinsic and apparent singularities in differentially flat systems, and application to global motion planning*, Systems & Control Letters **113** (2018), 117–124.

[17] _____, *On singularities of flat affine systems with n states and $n-1$ controls, international journal of robust and nonlinear control*, International Journal of Robust and Nonlinear Control **30** (2020), no. 9, 3547–3565.

[18] M.V. Kondratieva, A.V. Mikhalev, and E.V. Pankratiev, *Jacobi's bound for independent systems of algebraic partial differential equations*, AAECC **20** (2009), no. 1, 65–71.

[19] V.V. Krasil'shchik, V.V. Lychagin, and A.M. Vinogradov, *Geometry of jet spaces and nonlinear partial differential equations*, Gordon and Breach, New York, 1986.

[20] Harold W. Kuhn, *A tale of three eras: The discovery and rediscovery of the hungarian method*, Eur. J. Oper. Res. **219** (2012), no. 3, 641–651.

[21] Shun-Jie LI and Witold RESPONDEK, *A kinematic model of the nonholonomic n-bar system: Geometry and flatness*, IFAC Proceedings Volumes **43** (2010), no. 14, 689–694, 8th IFAC Symposium on Nonlinear Control Systems.

[22] George H. Lockwood, *Final report of the board of inquiry into air canada boeing 767 c-gaun accident — gimli, manitoba, july 23, 1983*, Tech. report, Canadian Government Publishing Center, 1985.

[23] Long K. Lu and Kamran Turgolu, *Differential thrust methodology for lateral/directional stability of an aircraft with a completely damaged vertical stabilizer*, International Journal of Aerospace Engineering **2018** (2018).

[24] Jean Lévine, *Analysis and control of nonlinear systems: A flatness-based approach*, Mathematical Engineering, Springer, 2009.

[25] _____, *On necessary and sufficient conditions for differential flatness*, Applicable Algebra in Engineering, Communication and Computing **22** (2011), no. 1, 47–90.

[26] Philippe Martin, *Contribution à l'étude des systèmes différentiellement plats*, Ph.D. thesis, Ecole Nationale Supérieure des Mines de Paris, Paris, France, 1992.

[27] _____, *Aircraft control using flatness*, CESA'96 – Symposium on Control, Optimization and Supervision (Lille, France), IMACS/IEEE-SMC Multiconference, 1996, pp. 194–199.

[28] Donald McLean, *Automated flight control systems*, Prentice Hall, New York, 1990.

[29] NATOPS, *NATOPS flight manual, navy model, F-4F aircraft*, 1978.

[30] François Ollivier, *Extending Flat Motion Planning to Non-flat Systems. Experiments on Aircraft Models Using Maple*, International Symposium on Symbolic and Algebraic Computation (ISSAC) (Lille, France), July 2022.

[31] _____, *Jacobi's bound: Jacobi's results translated in könig's, egerváry's and ritt's mathematical languages*, AAECC **2018** (2022).

[32] François Ollivier, *Looking for the order of a system of arbitrary ordinary differential equations*, AAECC **20** (2009), no. 1, 7–32.

[33] _____, *The reduction to normal form of a non-normal system of differential equations*, AAECC **20** (2009), no. 1, 33–64.

[34] François Ollivier and Brahim Sadik, *Jacobi's bound for a diffiety defined by a quasi-regular system*, Comptes Rendus Mathematique **345** (2009), no. 3, 139–144.

[35] François Ollivier and Alexandre Sedoglavic, *A generalization of flatness to nonlinear systems of partial differential equations. application to the command of a flexible rod*, IFAC Proceedings Volumes **34** (2001), no. 6, 219–223, 5th IFAC Symposium on Nonlinear Control Systems 2001, St Petersburg, Russia, 4-6 July 2001.

[36] P. Rouchon, M. Fliess, J. Lévine, and P. Martin, *Flatness and motion planning: the car with n trailers*, IN PROC. EUROPEAN CONTROL CONFERENCE, 1993, pp. 1518–1522.

[37] Timo Ströhle and Peter Betsch, *A simultaneous space-time discretization approach to the inverse dynamics of geometrically exact strings*, International Journal for Numerical Methods in Engineering **123** (2022), no. 11.

[38] Burak Yueksel, Gabriele Buondonno, and Antonio Franchi, *Differential flatness and control of protocentric aerial manipulators with any number of arms and mixed rigid-/elastic-joints*, 10 2016.

[39] Victor V. Zharinov, *Geometrical aspects of partial differential equations*, Series on Soviet and East European Mathematics, World Scientific, Singapore, 1992.